

DATE May 26, 2014**REFERENCE No.** 1313770115-003-TM-RevC-1000**TO** Joseph MacPhee
Public Works Government Services Canada (PWGSC)**CC** Steven Fiddler, Max Maxwell, and John Hull**FROM** Rob Luzitano, M.Sc.**EMAIL** rluzitano@golder.com**GEOPHYSICAL INVESTIGATION: GIANT MINE TAILINGS, YELLOWKNIFE, NWT****1.0 INTRODUCTION AND OBJECTIVES**

Golder Associates Ltd. (Golder) has conducted a geophysical investigation for PWGSC at the Giant Mine in Yellowknife, NWT using multiple methods. The primary objective of the survey was to map variations in bedrock depth beneath the tailings based on electrical resistivity using a form of the electrical resistivity imaging (ERI) method. The desired outcome was to establish thickness of overburden over bedrock, and bedrock topography, in order to help guide the ongoing reclamation efforts. The surveys were carried out at the site's Tailings Storage Facilities (TSF); in particular, the North, Central, South, and Northwest Ponds.

The second objective of the survey was to map buried metal objects within the Central Pond in an area believed to be used historically as a landfill for industrial metal waste.

Field work for the investigation was conducted from March 5 to 9, 2014. This report presents the basic principles of the geophysical methods used, documents the surveys, and discusses the survey results and interpretation.

2.0 GEOPHYSICAL METHODS

Based upon our understanding of the site and the physical contrasts between bedrock and overburden (tailings in particular), electrical resistivity was chosen as the primary target property. While seismic refraction is often a more robust method for profiling bedrock, electrical resistivity imaging (ERI) can often image the bedrock more quickly and easily (and potentially at greater resolution of features); therefore, seismic refraction was reserved as a back-up (and significantly slower) method, in particular, to possibly use in areas where bedrock was suspected to be deeper. Additionally, considering that the frozen ground conditions precluded the more typical—and deeper sounding—electrical resistivity imaging (ERI) survey that uses electrode stakes inserted into the ground, the ERI survey was carried out using a capacitively-coupled electrical resistivity imaging (C-CERI) system that can be towed behind an Argo. The primary limitation for C-CERI compared to staked-ERI is the investigation depth, which was anticipated to possibly be limited to approximately 10 m or less; however, depending on the electrical conductivity of the tailings overburden, depths approaching 15 m could be possible. These possible depth ranges were, however, within the primary depth range of interest.



The subsequent bedrock depth interpretation was anticipated to require calibration from borehole and/or test pit logs to confirm/adjust actual depths. This calibration would use existing logs and excavation information.

All of the survey areas (North, Central, South, and Northwest Ponds) were surveyed with C-CERI where accessible. Seismic refraction was tested in the middle of the South Pond where preliminary C-CERI profiles indicated deeper bedrock.

The second objective—delineating areas of buried metal debris—was achieved by carrying out a magnetic gradiometer survey in a section of Central Pond.

The following sections discuss, in more detail, the basic principles of the geophysical methods used in this investigation.

2.1 C-CERI METHOD

Resistivity of soil and rock depends, in part, on the constituent materials (Table 1). Primary factors controlling resistivity typically include grain size, porosity, rock-type, temperature, ice content and water saturation. Some examples follow.

- Clays and silts are conductive (low resistivity) compared to sands and gravels (high resistivity);
- Fresh water saturation within clay-free soils reduces resistivity in accordance with Archie's Law, i.e., water-saturated sands have a lower resistivity than dry sands;
- Increasing the concentration of total dissolved solids (TDS), particularly salts and metals, in contained groundwater normally reduces resistivity significantly;
- The presence of organic materials tends to increase the matrix resistivity; and
- Liquid water tends to decrease resistivity, whereas high ice content significantly increases soil resistivity.

Table 1: Resistivity and Conductivity Ranges for Common Geologic Materials

Material	Resistivity (ohm-m)	Conductivity (mS/m)
Fresh Water	2,000	0.5
Sea Water	0.033	30,000
Dry Sand	100,000	0.01
Saturated Sand	100 - 5,000	0.2 - 10
Gravel	100 - 10,000	0.1 - 10
Silts	10 - 1,000	1 - 100
Clays	1 - 500	2 - 1,000
Granite	1,000 - 100,000	0.01 - 1
Limestone	500 - 2,000	0.5 - 2
Shale	10 - 1,000	1 - 100
Ice	100,000	0.01

Table created by: JKW

Checked by: RDL

The OhmMapper TRN 5 survey instrument, manufactured by Geometrics Inc., is a C-CERI system designed to measure subsurface resistivity, both laterally and vertically, without the use of electrodes traditionally employed in direct current systems. The technique is, therefore, not susceptible to many of the limitations encountered by electrode-based direct current systems, such as problems resulting from the high contact resistance that commonly occur between the electrodes and frozen soils.

The OhmMapper system consists of an ungrounded transmitter, a receiver array of up to five receivers, and a data logger. An alternating current is coupled to the ground by the transmitter, inducing a current to flow within the ground. This secondary current, in turn, couples a current to the receiver array. The voltage that is measured by the receivers is proportional to the resistivity of the earth between the transmitter and receiver array.

The transmitter and receiver array are typically pulled along the ground by a truck, an all-terrain vehicle, or by an operator on foot, collecting near-continuous data. Data are recorded by means of a digital data logger through a fibre optic cable connected to the receiver array and are positioned in real time by a Global Positioning System (GPS) receiver. Figure 1 displays a typical field configuration for the OhmMapper towed by an Argo. Multiple passes are typically made along the same survey line using different spacing between the transmitter and receiver array, thereby providing varying depths of investigation. Investigation depth is largely controlled by the transmitter-receiver separation and the electrical properties of the ground, where increasing the distance between the transmitter and receiver increases penetration depth. However, the maximum viable transmitter-receiver separation is controlled by the ground conductivity, where an increase in ground conductivity tends to reduce the maximum separation and so reduces the maximum depth of investigation. Clay-rich soils and groundwater high in TDS can, therefore, limit signal penetration.

The instrument geometry used for the TSF was a receiver and transmitter dipole length of 20 m, with a transmitter/receiver distance of 5 m. The exception to this array geometry was the north pond, where dipole lengths of 10 m and transmitter/receiver distance of 3 m were initially used on the survey lines to assess tailings thickness. The lines were subsequently re-surveyed with the longer geometry to increase exploration depth.

Resulting data were processed using an OhmMapper system software and were modelled using the Res2DInv inversion modelling software by Loke.



Figure 1: OhmMapper Field Configuration

2.2 SEISMIC REFRACTION METHOD

In the seismic refraction method, an acoustic wave is generated at the surface which propagates radially into the subsurface. On encountering boundaries between media having contrasting mechanical properties, including density, elasticity and consequently seismic velocity, the incident wave pulse is partially reflected and partially transmitted into underlying strata (Figure 2). The ray-path of the incident-transmitted pulse is bent, or refracted, at the boundary in accordance with Snell's law. In particular, if seismic velocity increases across the boundary, the ray-path is refracted toward the boundary. As the angle of incidence increases, so does the angle of refraction until for some critical incidence angle, depending on the relative seismic velocities, the refracted wave pulse travels along the boundary and acts as a moving source of secondary wave pulses which propagate upward into overlying strata as refraction-head waves. The refraction-head waves ultimately reach the surface where their arrival is detected by a linear array of geophones. By measuring the elapsed time between initial pulse generation at the shot-point and subsequent arrival of critical refraction-head waves at successively more distant geophones, relatively straight-forward calculations yield estimates of layer velocities and thicknesses. In general, seismic interpretation methods assume the existence of relatively shallow-dipping layered geology with increasing layer velocities at increasing depth.

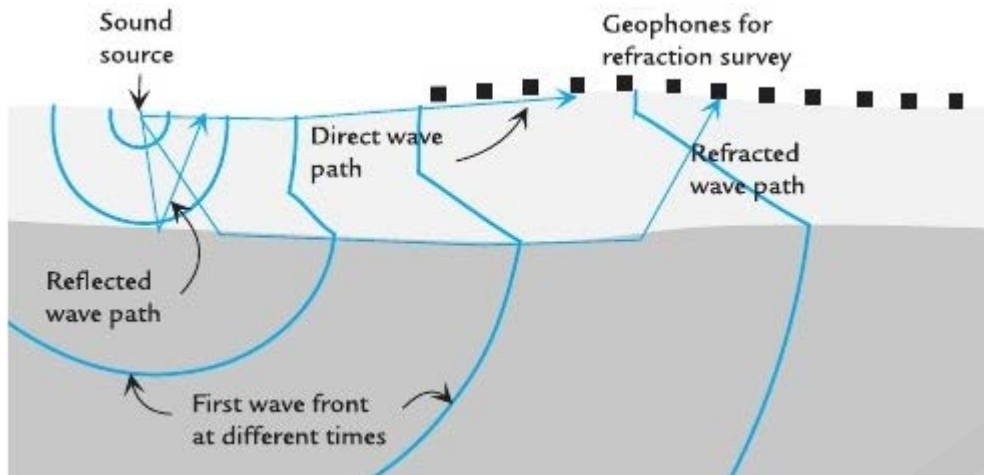


Figure 2: Seismic Refraction Method

Ranges of compression, or P-wave, velocities for representative earth materials are listed in Table 2.

Table 2: Approximate Range of Seismic Velocities for Typical Earth Materials (Redpath, 1973)

Material	Seismic P-wave Velocity Range [m/sec]
Weathered Surface Material	305 - 610
Gravel, rubble, or sand (dry)	468 - 915
Clay	610 - 1,830
Sandstone	1,830 - 3,970
Shale	2,750 - 4,270
Limestone	2,140 - 6,100

Typically, seismic depth determinations are accurate to within 10-20%, subject to the assumptions of refraction techniques including:

- layered subsurface;
- generally, layer slope variations of less than 20 degrees; and
- velocities increase with depth and relatively gradual changes in layer topography.

A 24 channel Geometrics Geode seismic system, with twenty-four 10Hz geophones placed at a spacing of 5 m, was used to collect the survey data. A percussion source (sledge hammer striking a metal base plate) was tested and subsequently used for the survey.

2.3 MAGNETIC METHOD

A magnetometer is used to measure the magnetic flux density of the Earth's magnetic field. Some materials - such as iron, nickel, cobalt and alloys containing these materials (known as *ferromagnetic* materials) - will distort the natural surrounding magnetic flux density by adding to, or subtracting from, the ambient magnetic field. The magnetic method operates on the principle that, in the presence of ferromagnetic materials, this localized distortion of Earth's total magnetic field may be measured by a magnetometer. Man-made objects, such as pipelines and conduits, often contain iron and so may be detectable by a magnetic survey. Several different types of magnetometers are commonly used in magnetic surveys - including proton precession, fluxgate and alkali vapour (or Overhauser) magnetometers. The main advantages of Overhauser magnetometers are high-sensitivity, an omni-directional sensor and short measurement recovery times.

Magnetic survey data are acquired by moving the magnetometer along a traverse and measuring the total magnetic field at a number of discrete locations along the survey line. Multiple survey lines within an area are often combined to present a magnetic map of the entire survey area. Localized magnetic anomalies due to buried ferromagnetic materials often exhibit a characteristic high-value response flanked by anomalously low-value response. Linear utilities may be identified by a succession of anomalously high and low-value readings oriented in a straight line in an areal map view.

For this survey, a GEM Overhauser GSM-19 gradiometer was used. Gradiometers are multiple-sensor magnetometers that are able to measure the difference, or gradient between the vertically spaced sensors, allowing greater horizontal resolution of anomalous bodies, particularly at shallow depths. A vertical sensor spacing of 0.57 m was used for this survey. Positions of the survey stations were collected and digitally recorded using an integrated GPS receiver. The sampling frequency chosen for the survey was 2 Hz. The resulting gradient data were gridded, contoured and plotted using the Golden Surfer v11 contouring program. As geophysical survey data are commonly irregularly spaced, trends that are suggested in the data are generally best expressed using the kriging geostatistical gridding method.

3.0 RESULTS

Results of the geophysical investigation are discussed for each of the three methods in separate sections below. Data quality from all three surveys was generally good to excellent. Coverage of the different surveys is shown in Figures 3 and 4.

Figure 3 displays the survey line locations as projected onto a Google Earth image of the North, Central and South TSF Ponds. Seismic refraction data were collected exclusively along one line (Line 11) located in the South Pond, magnetic data were collected exclusively in the Central Pond area, and C-CERI data were collected in all three pond areas. The Central Pond C-CERI survey area was bounded by deep drainage features west and south of the lines, as well as a large surface storage area for sea-cans located to the northeast. Central Pond is also bounded to the south by an access road where bedrock outcrops.

Figure 4 displays the C-CERI survey line locations as projected onto a Google Earth image of the Northwest TSF Pond. No magnetic or seismic data were collected in the northwest pond area.

All positional data are presented in the Giant Mine local grid coordinate system (GMRP) in metres.

3.1 C-CERI RESULTS AND INTERPRETATION

Resulting C-CERI profiles are presented in Attachment A (Figures A-1 – A-5) as colour contoured 2-D profiles of modelled resistivity. Resistivity is represented in a colour scale, with low resistivities appearing as cool colours (blue, green) and high resistivities as hot colours (yellow, red).

While results varied at each of the pond survey areas, the general trend was a layer of higher resistivity material overlying lower resistivity material. The highest resistivity values were generally located in the upper 2 - 5 m of the subsurface and ranged from approximately 100 – 500 ohm-m. This upper layer of higher resistivity is attributed to a combination of seasonal frost and reduced liquid water saturation. Test pit and borehole information previously collected at the site indicates that soils are drier near the surface with water saturation increasing with depth. Near topographical lows and in proximity to surface pond water, however, this shallow resistor is generally thinner and with relatively lower resistivity. Therefore, the thickness and magnitude of the surface resistor may be an indicator of unhydrated material, seasonal frost, and or permafrost. Lateral variation of material grain size may also be a factor, as fine-grained soils generally reduce resistivity.

Below the shallow resistive layer seen in all the areas surveyed, a relatively sharp reduction in resistivity is evident. It is possible that this reduction is due to increased water saturation of the material and/or the absence of frost/permafrost. Once again, soil grain size may be a contributing factor, where grain-size would generally reduce with depth. The bulk of this lower resistivity layer has a much narrower range of resistivity, generally less than 50 ohm-m.

The objective of the survey was to identify the bedrock surface underlying the overburden soils. Bedrock was anticipated to appear as a relative resistor underlying the more conductive overburden layer. While a third, more resistive, layer was identified in portions of the areas surveyed - particularly adjacent to bedrock outcrops and near the edges of the ponds - in general, no deep continuous resistive layer was identified in the middle of the ponds. This is likely due to bedrock depths that are greater than the exploration limits of the method (approximately greater than 15 m). The low resistivity material layer (<50 ohm-m) predominates the profiles at maximum exploration achieved in all ponds surveyed, indicating thicker low resistivity overburden material, and therefore greater depth to resistive bedrock. This finding is consistent with the information recovered from the few boreholes available in the area, where bedrock was only encountered in GA11-T-02 and other boreholes were drilled to approximately 14 to 16 m without encountering bedrock. Additionally, it is likely that the native soil resting on bedrock would have similar electrical properties to tailings material, so the estimated overburden thickness includes any sequence of native soils as well. Some sections do exhibit an increase in resistivity with depth, possibly indicating bedrock within the exploration limits; the best example is the profile of Line 15 in the South Pond (Figure A-1). Calibration with borehole logs and the subsequent interpretation of the bedrock surface is discussed further in the following section.

3.1.1 Bedrock Interpretation from C-CERI Profiles

Four pre-existing boreholes were located within the areas of the ponds that were surveyed: two in the South Pond (GA11-T-01 and GA11-T-02); one in the Central Pond (GA11-T-04); one in the North Pond (GA11-T-11); and none in the Northwest Pond. As noted above, within the 9 to 16 m depths spanned by the boreholes, only GA11-T-02 (in the South Pond) encountered bedrock. As indicated on the profile of Line 14 (Figure A-1), borehole GA11-T-02 is located approximately 16 m west of the profile within a section of Line 14 that does exhibit a significant higher resistivity layer beneath the lower resistivity overburden. Bedrock depth indicated by the borehole log correlates with the top of the resistivity gradient where resistivity begins to increase

with depth. Although the borehole appears to be located adjacent to a steep bedrock slope, similar correlations (top of gradient) have been observed at other sites having higher resistivity bedrock beneath low resistivity overburden. Based on this single borehole correlation, the bedrock interface was interpreted and digitized as indicated by the red dashed lines on the profiles in Figures A-1 through A-5.

As noted above, within much of the ponds (beyond 25-50 m from their bedrock “shores”) bedrock is interpreted to occur deeper than the approximately 15 m depth of exploration of the C-CERI profiles.

Resulting interpreted bedrock depths are also plotted in map view on air-photographs and provided as Figures 5 to 7. Bedrock depths are plotted as colour shaded circles along the survey tracklines where hot colours (red to yellow) correspond to approximately 1 – 10 m depth and cool colours (yellow-green to green-blue) correspond to approximately 10 – 15 m depth. Depths greater than 15 m (from the OhmMapper profiles) are indicated by purple shading.

The colour bar of the bedrock depth maps continues to dark blue at approximately 20 m since depths of up to 23 m are included from the seismic spread on Line 11 in the South Pond (Figure 5).

3.2 SEISMIC REFRACTION RESULTS

The seismic refraction survey is presented as a profile of the interpreted bedrock depth in the TSF South Pond (Figure 8). The interpreted average velocity of the bedrock is 3325 m/s, with overburden velocity ranging from 600 - 1800 m/s. The profile coincides approximately with the eastern two-thirds of C-CERI Line 11 (Figure 5). The profile indicates interpreted bedrock depth ranging from 18 to 23 m east of GMRP 33605 E. Bedrock depth west of GMRP 33605 E is less than 18 m sloping upwards to the west to a depth of 11 m at 36589 E. The eastern half of the line correlates reasonably with the C-CERI profile, while the western portion suggests a resistive boundary should be visible within the C-CERI profile, and it is not (see also Figure A-1 in Attachment A). This discrepancy could be due to a harder, and lower resistivity, till layer within this section; and, therefore, not actually bedrock. An additional till layer could also account for the more complex seismic signal observed across the western portion of the seismic spread.

3.3 MAGNETIC RESULTS

The gradiometer survey data are presented in Figure A-6, of Attachment A, as a colour-shaded contour map of measured magnetic gradient over the surveyed area in TSF Central Pond, as well as a map of interpreted locations of metals based upon magnetic gradient deviations greater than 75 nT/m. The interpretation map is also provided at a larger scale overlaid on an air photograph as Figure 9. The interpretation map shows a large number of metallic objects and concentrations of objects. The survey area includes a large surface drainage channel trending southwest to northeast, located near the centre of the survey area and in the area of the most closely spaced survey lines. The channel area is characterized by a relative lack of large magnetic gradient responses and, therefore, is interpreted to contain fewer metallic objects.

The area northwest of the channel was a bench 3 – 4 m higher in elevation, with many metal objects visible on the surface. The observed magnetic gradient in this area is generally higher due to the proximity of the metals to the sensors. It should be noted that the surface metal (or shallow buried metal) may mask the response from deeper buried metal.

The area east and south of the channel is also higher in elevation. No surface metal objects were observed in this area. The area immediately adjacent to the east of the channel is characterized by an apparent long linear magnetic gradient anomaly, suggesting a linear metallic object such as a cable; however, this interpretation is more speculative due to the gap in data coverage through the channel. The southern portion of the survey area is characterized by several localized anomalous magnetic gradient responses attributed to buried metallic objects.

4.0 SUMMARY AND RECOMMENDATIONS

Golder has conducted a geophysical investigation for PWGSC at the Giant Mine in Yellowknife, NWT to establish the depth of bedrock within the site's North, Central, South and Northwest Tailings Ponds primarily by using the C-CERI method. The second objective of the survey was to map metal objects by using a gradiometer within the Central Tailings Pond in an area believed to be used historically as a landfill for industrial metal waste. Field work for the investigation was conducted from March 05 to 09, 2014.

The C-CERI results indicate that bedrock is likely deeper than the maximum exploration depth of the instrument for the majority of the area surveyed (greater than approximately 15 m), and particularly in the centre of the TSF ponds. The notable exceptions (shallower bedrock) were found nearer the perimeter of the ponds and near bedrock outcrops, and along Line 15 near the east side of the South Pond. Results of the limited seismic refraction survey generally agreed with the results of the C-CERI survey.

The gradiometer survey interpretation identified extensive areas where buried metal likely exists; the response was also affected in those areas where metallic debris was observed at surface in the vicinity of the TSF Central Pond.

Should profiles of deeper bedrock topography be required, recommendations for further work—during thawed ground conditions—could include an electrical resistivity imaging (ERI) survey and/or a more extensive seismic refraction survey. The ERI method is able to penetrate much deeper than the C-CERI method employed, and, based on the resistivity contrast between the overburden materials and bedrock observed during this investigation, an ERI survey would likely be able to image the bedrock contact at depths greater than 15 m. A more extensive seismic refraction survey would likely also be able to image the bedrock contact at depths greater than 15 m with the added suggestion that a seismic source more powerful than a sledge hammer and steel plate be employed. Finally, additional boreholes (or other intrusive method) that intersect bedrock located on the geophysical lines, especially in the deep bedrock areas, would improve the calibration of the geophysical interpretation for bedrock depth.

5.0 CLOSURE

We trust this technical memorandum provides the information required at this time. Should there be any questions or comments, please contact the undersigned.

GOLDER ASSOCIATES LTD.

Robert Luzitano, M.Sc.
Senior Geophysicist

Mark Bowman, P.Geoph. (AB)
Associate, Senior Geophysicist

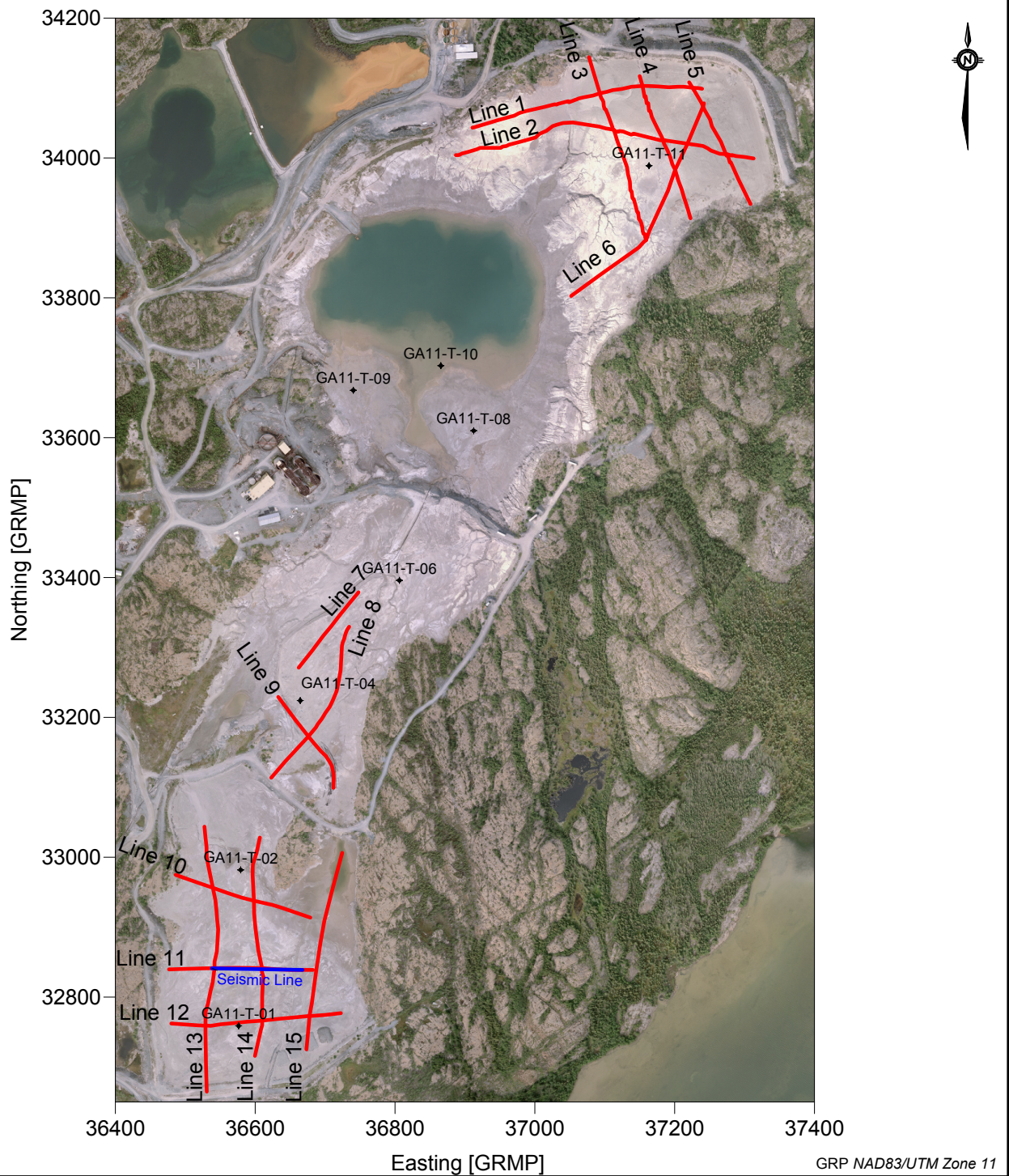
RL/MB/rs/lr

Attachments Figures 3 to 9
 Attachment A: Figures A1 to A6

o:\final\2013\1377\13-1377-0115\1313770115-003-tm-revc-1000\1313770115-003-tm-revc-1000-pwgsc tech memo 27may_14.docx

DRAFT

DRAFT



LEGEND

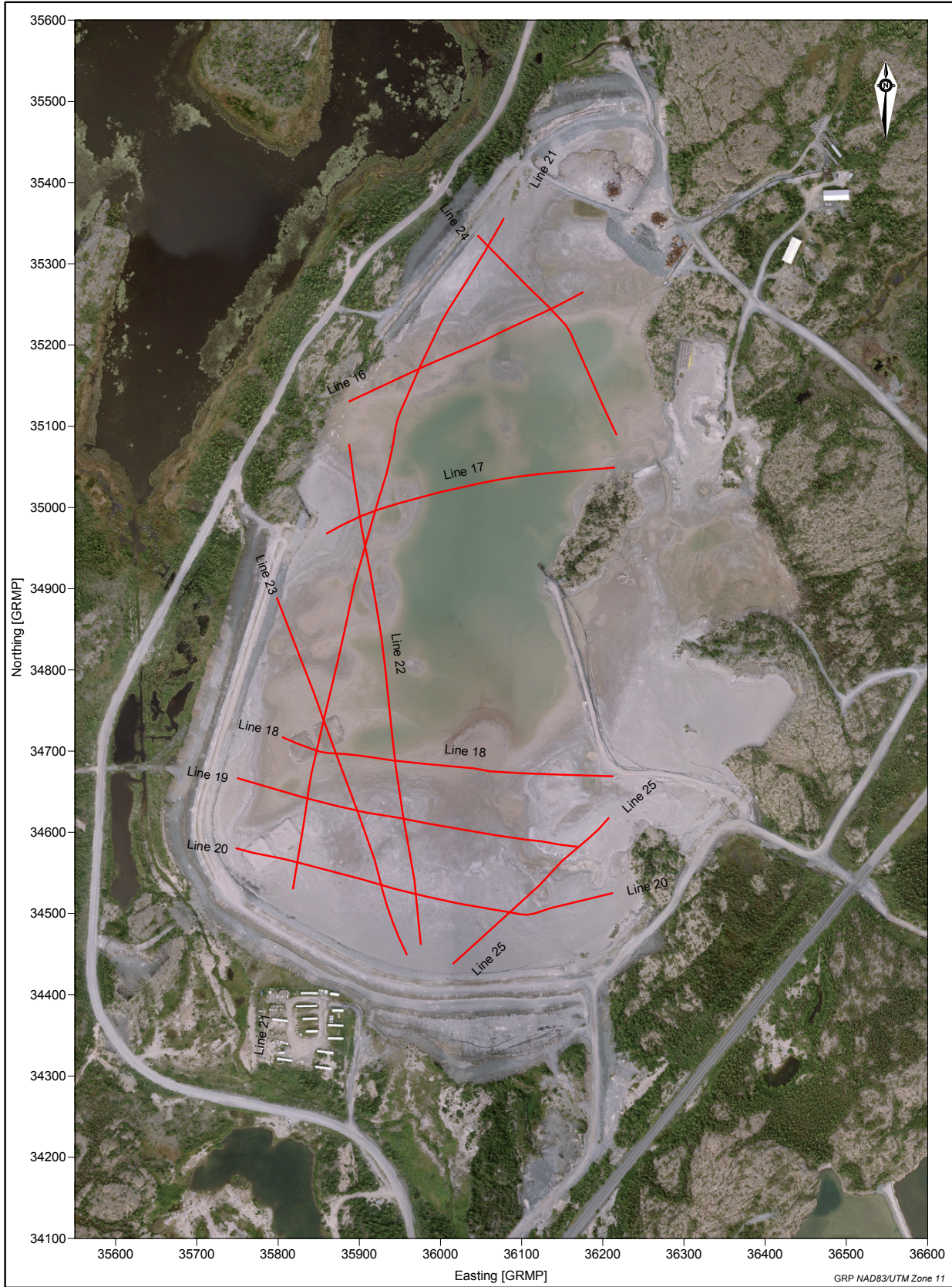
- C-CERI Survey Lines
- Seismic Refraction Line
- Gradiometer Survey Track
- ◆ Borehole

CLIENT
PWGSC
Giant Mine, Yellowknife, NT

TITLE
**Geophysical Investigation
Tailings Storage Facilities (TSF)
North, Central and South Ponds
Survey Line Location Map**



PROJECT	13-1377-0115		
DESIGN	JG	22MAR14	NOT TO SCALE
REVIEW	MB	7APR14	
			FIGURE: 3

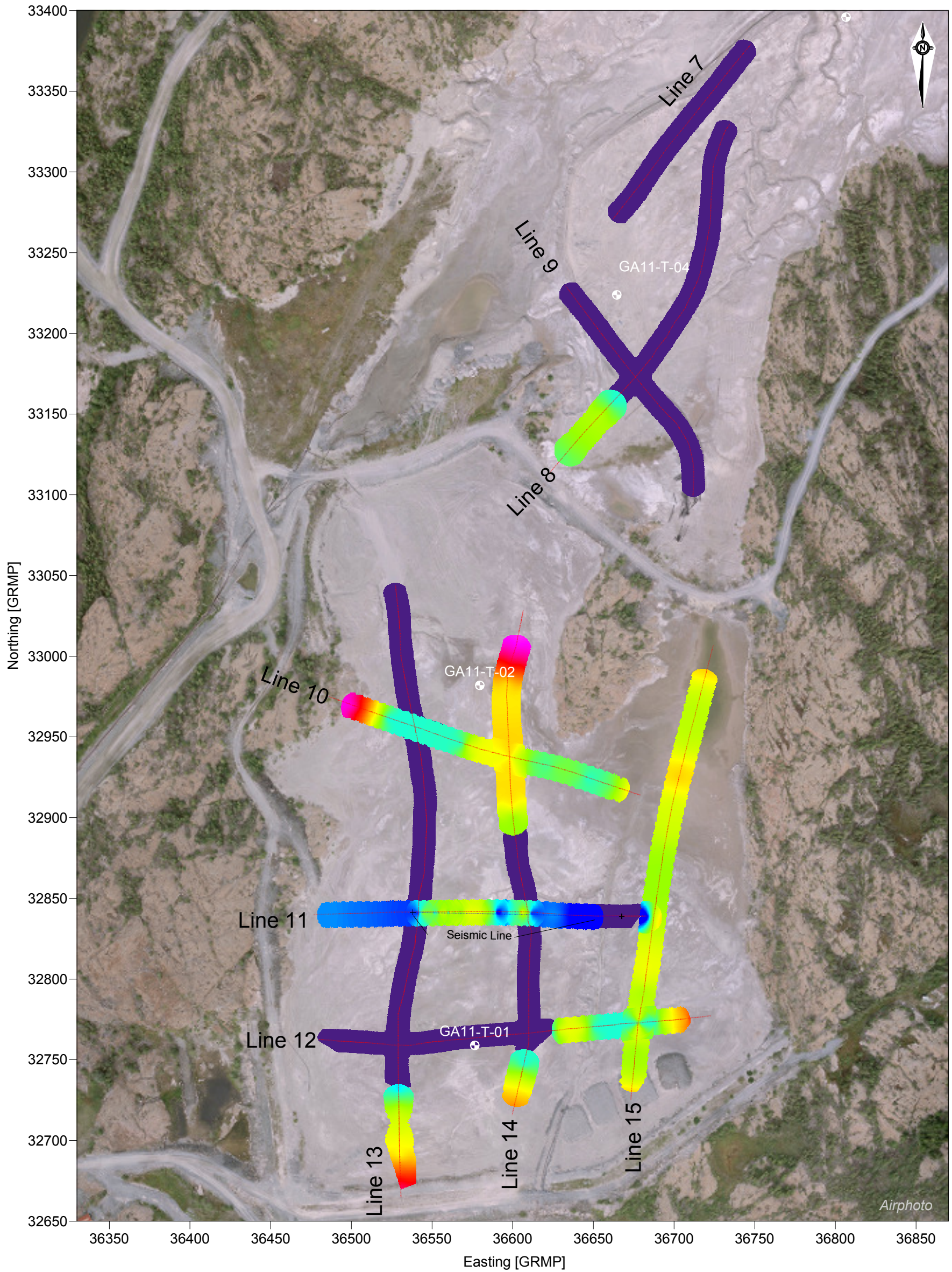


LEGEND

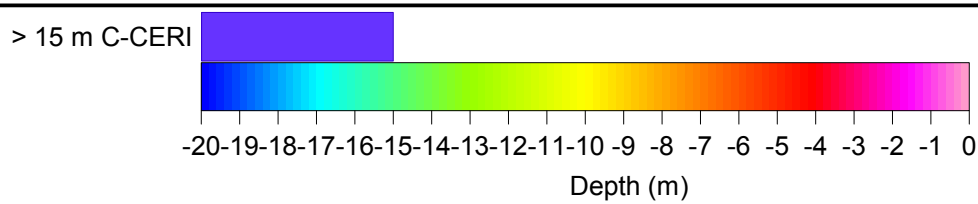
— C-CERI Survey Lines

CLIENT		PWGSC Giant Mine, Yellowknife, NT	
TITLE		Geophysical Investigation Tailings Storage Facilities (TSF) Northwest Pond Survey Line Location Map	
PROJECT	13-1377-0115	NOT TO SCALE	
DESIGN	JG 22MAR14	FIGURE: 4	
REVIEW	MB 7APR14		






GRP NAD83/UTM Zone 11

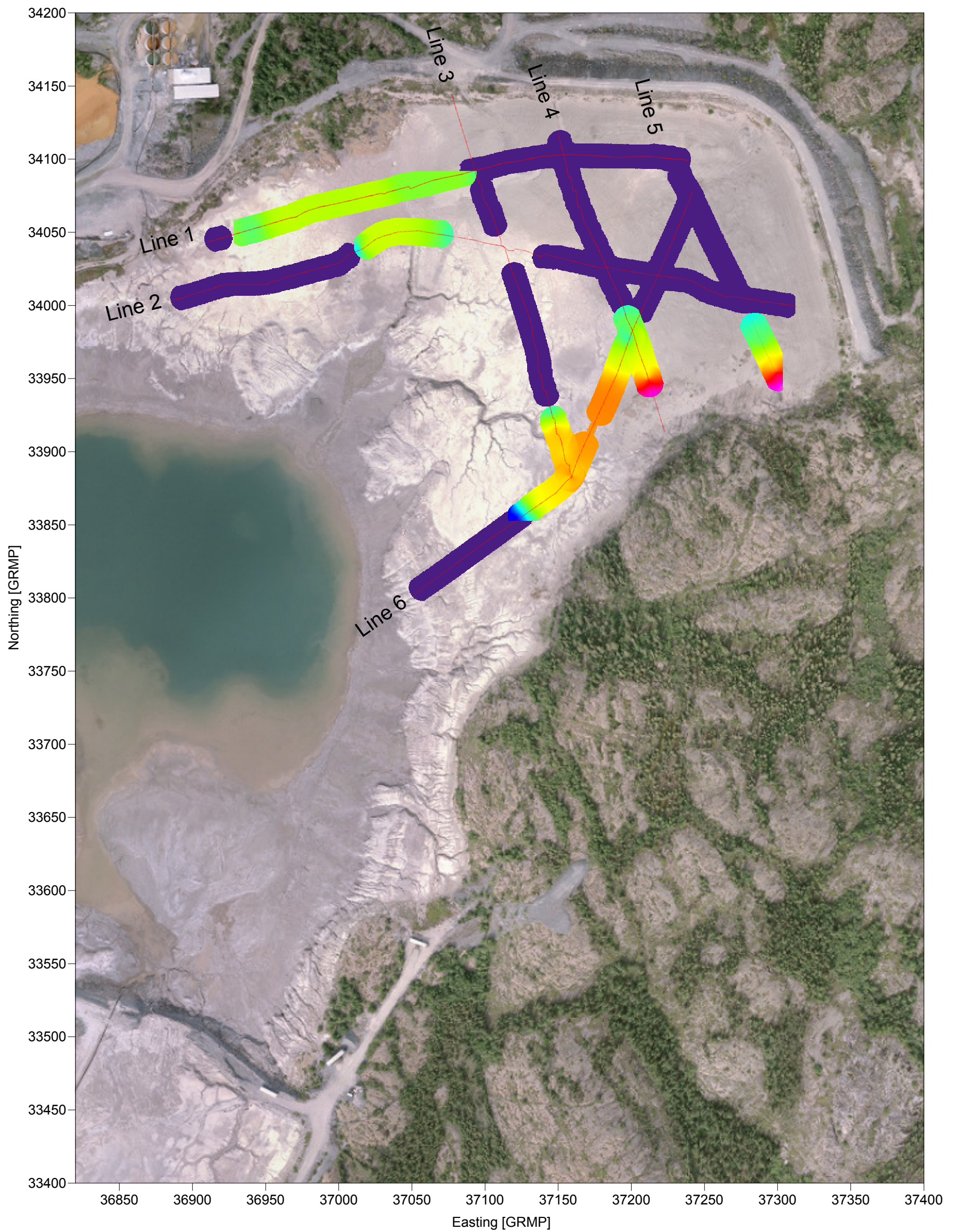


LEGEND

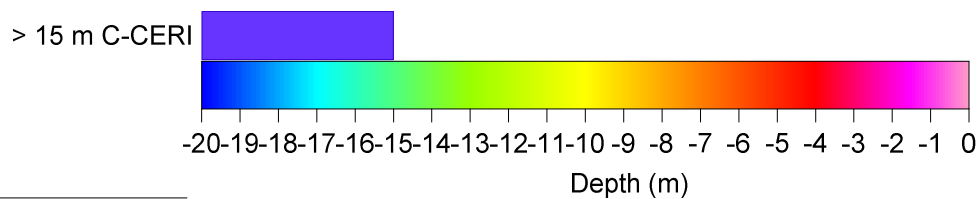
- C-CERI Survey Lines
- + Borehole

DRAFT

CLIENT		PWGSC Giant Mine, Yellowknife, NT	
TITLE			
Geophysical Investigation Tailings Storage Facilities (TSF) Central and South Ponds Survey Line Locations and Interpreted Bedrock Depth			
 Golder Associates Calgary, Alberta	PROJECT	13-1377-0115	
	DESIGN	JG 22MAR14	NOT TO SCALE
	REVIEW	MB 7APR14	
			FIGURE: 5



GRP NAD83/UTM Zone 11

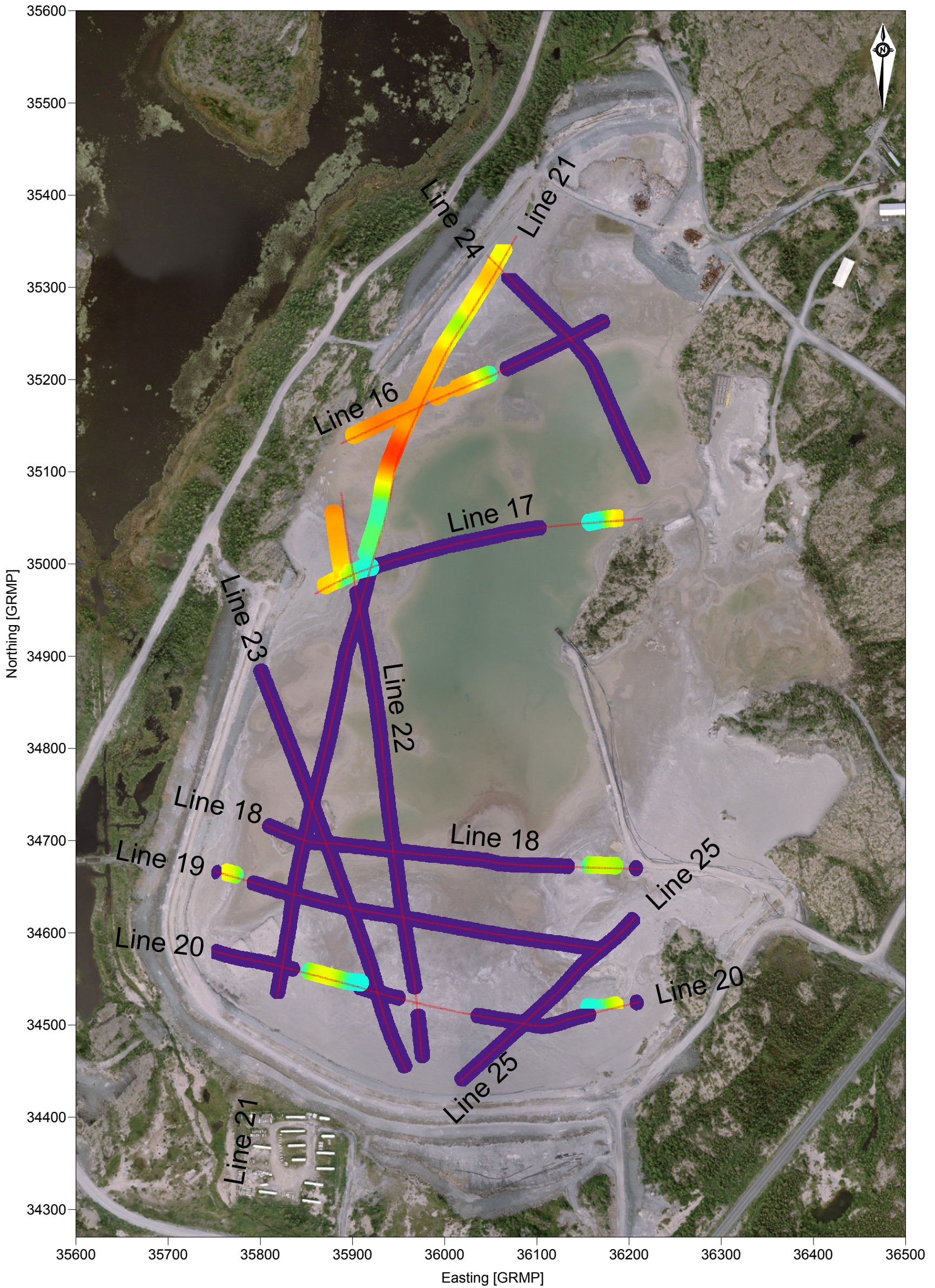


LEGEND

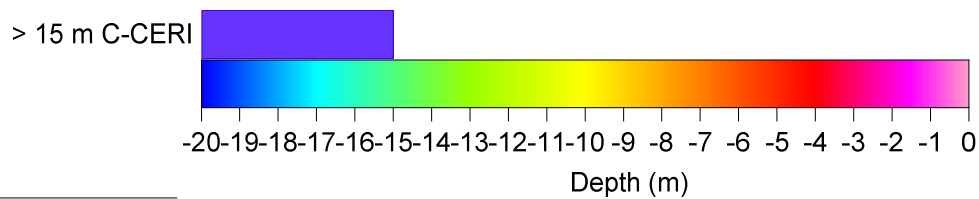
- C-CERI Survey Lines
- ◆ Borehole

DRAFT

CLIENT	PWGSC Giant Mine, Yellowknife, NT		
TITLE	Geophysical Investigation Tailings Storage Facilities (TSF) North Pond Survey Line Locations and Interpreted Bedrock Depth		
 Golder Associates Calgary, Alberta	PROJECT	13-1377-0115	
	DESIGN	JG	22MAR14
	REVIEW	MB	7APR14
			FIGURE: 6



GRP NAD83/UTM Zone 11

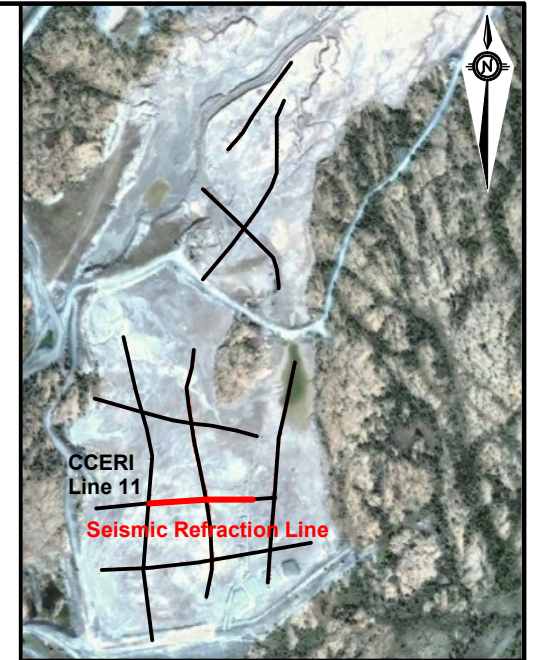
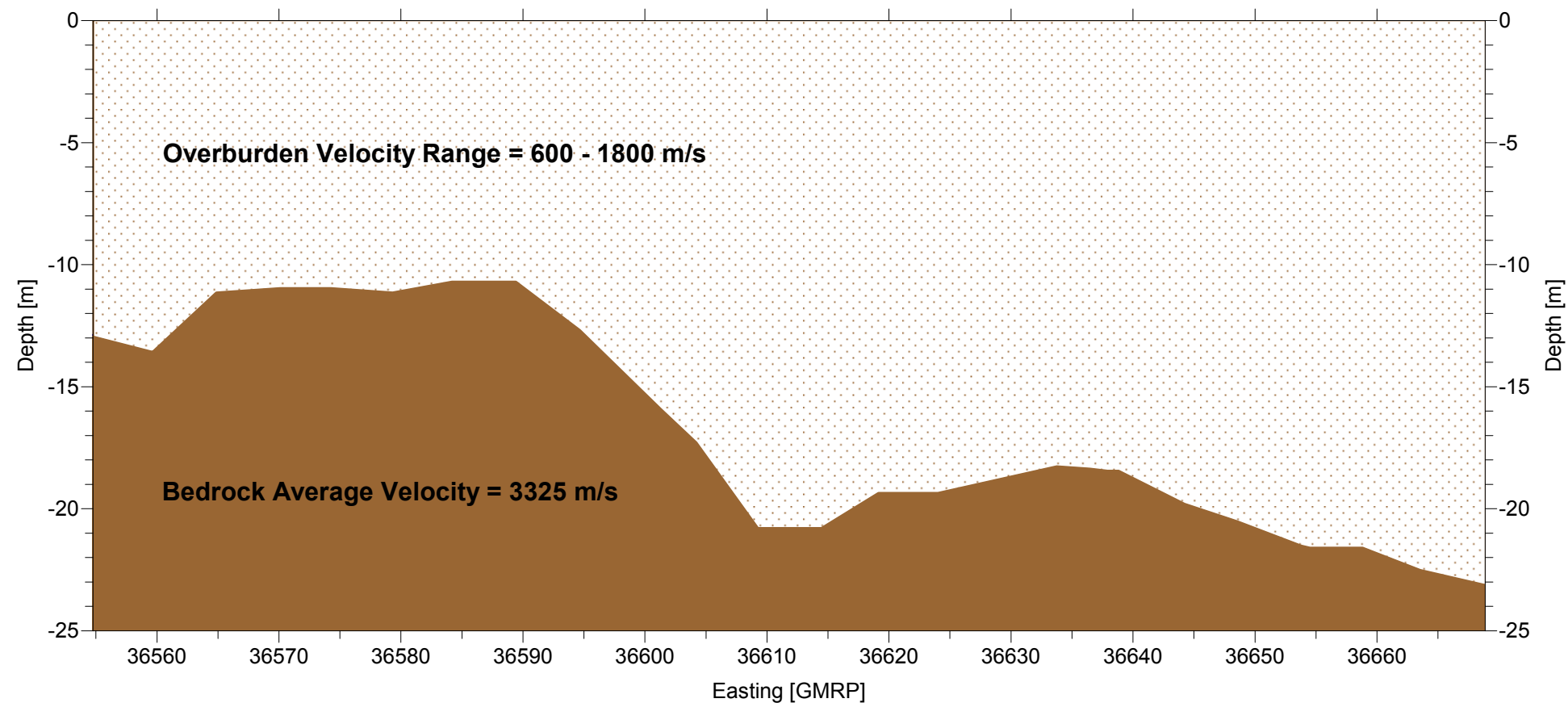


LEGEND

- C-CERI Survey Lines
- ◆ Borehole



DRAFT


CLIENT	PWGSC Giant Mine, Yellowknife, NT		
TITLE	Geophysical Investigation Tailings Storage Facilities (TSF) Northwest Pond Survey Line Locations and Interpreted Bedrock Depth		
 Golder Associates Calgary, Alberta	PROJECT	13-1377-0115	
	DESIGN	JG	22MAR14
	REVIEW	MB	7APR14
			FIGURE: 7

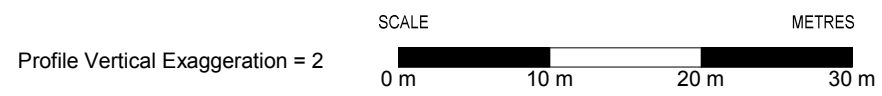


DRAFT

LEGEND

-  Interpreted Overburden Layer
-  Interpreted Bedrock Layer

CLIENT	PWGSC Giant Mine, Yellowknife, NT		
TITLE	Geophysical Investigation Tailings Storage Facilities (TSF) South Pond Seismic Refraction Interpreted Bedrock Depth		
	PROJECT	13-1377-0115	
	DESIGN	JG 22MAR14	SCALE AS SHOWN
	REVIEW	MB 7APR14	FIGURE: 8

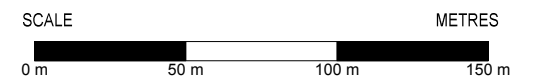




DRAFT

LEGEND

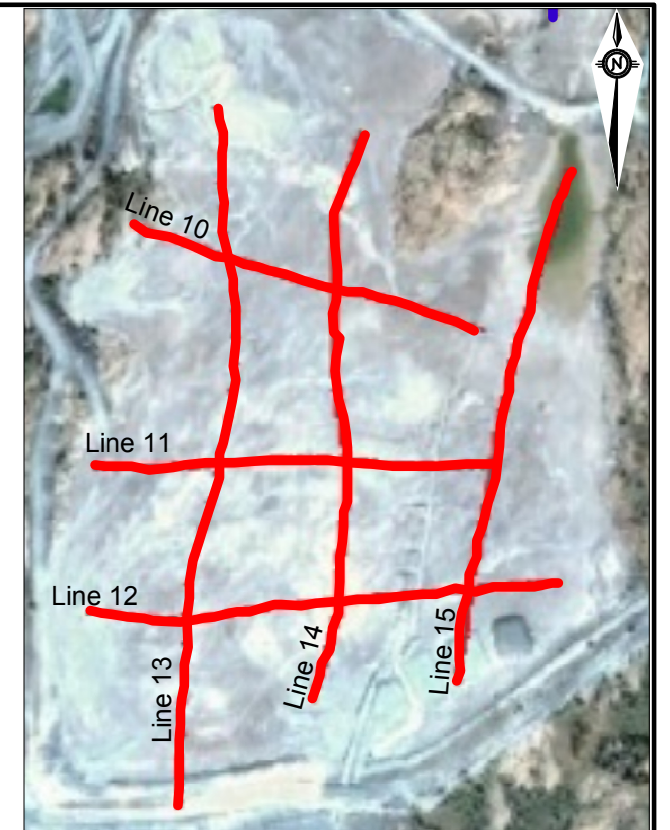
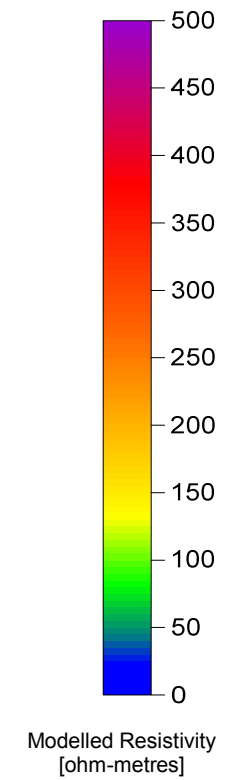
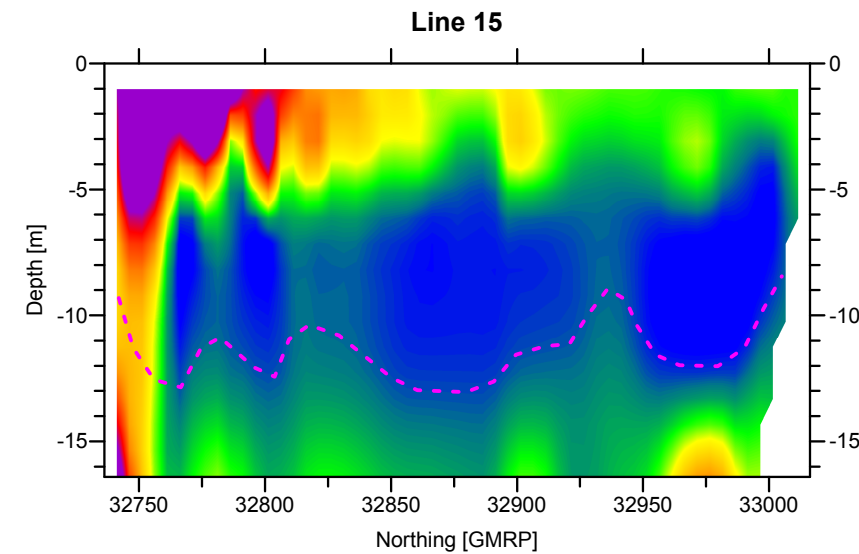
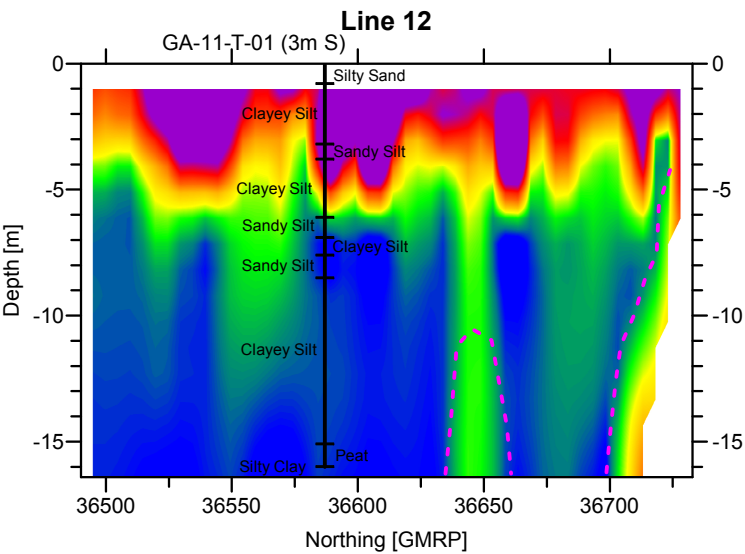
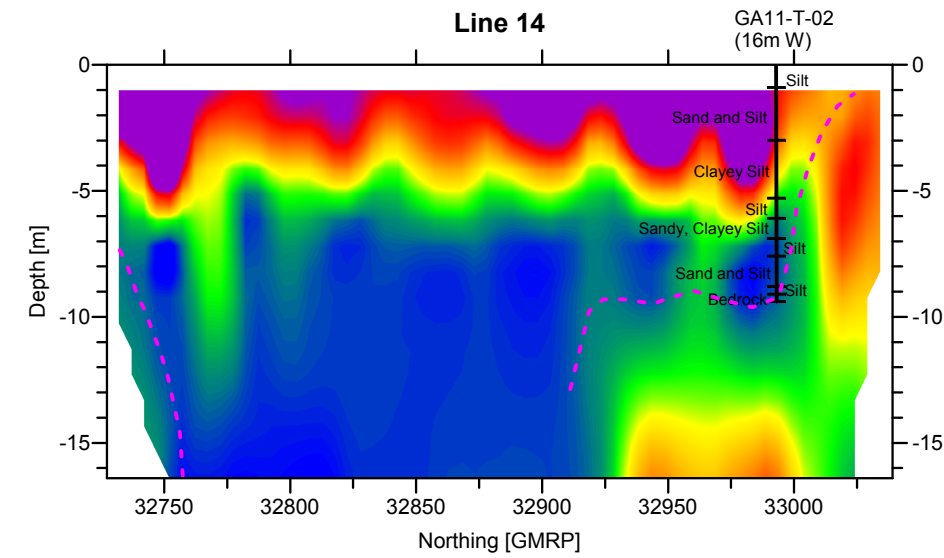
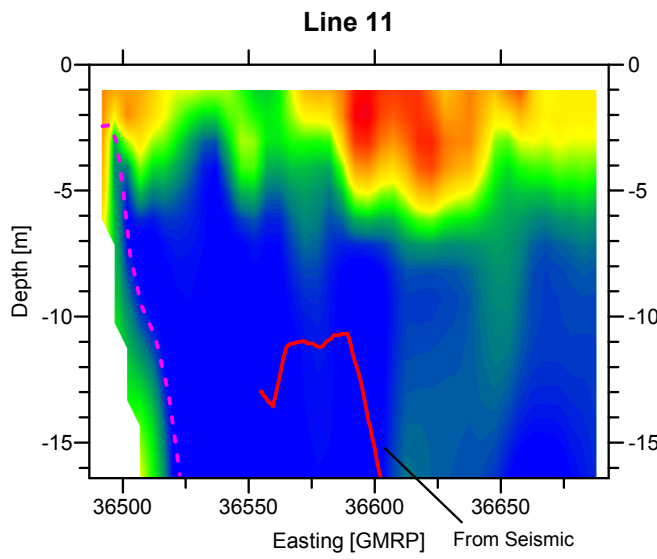
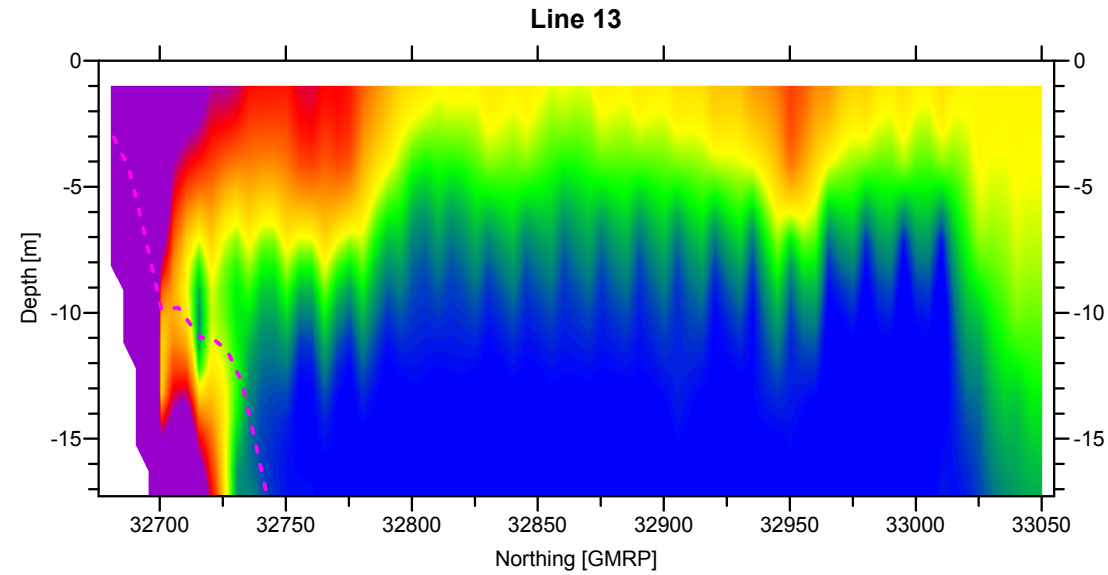
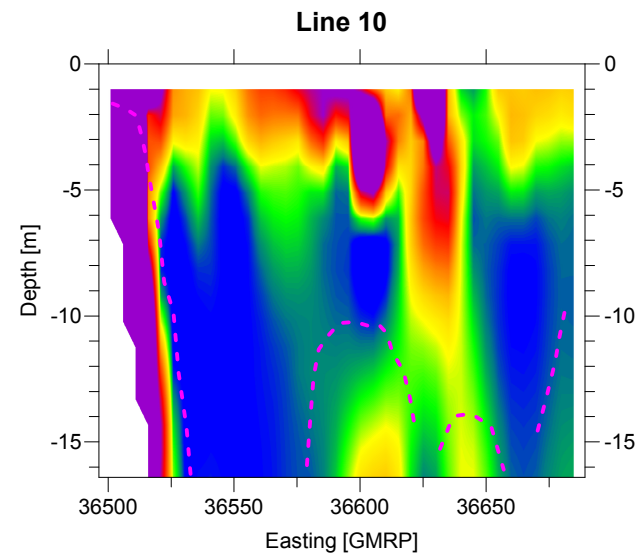
- Gradiometer Survey Track
- Interpreted Location of Buried Metal
- Borehole




<small>CLIENT</small>	PWGSC Giant Mine, Yellowknife, NT		
<small>TITLE</small>	Geophysical Investigation Tailings Storage Facilities (TSF) Central Pond Interpreted Vertical Gradient Map		
 Golder Associates <small>Calgary, Alberta</small>	<small>PROJECT</small>	13-1377-0115	
	<small>DESIGN</small>	JG	22MAR14
	<small>REVIEW</small>	MB	7APR14
	<small>SCALE AS SHOWN</small>	FIGURE: 9	

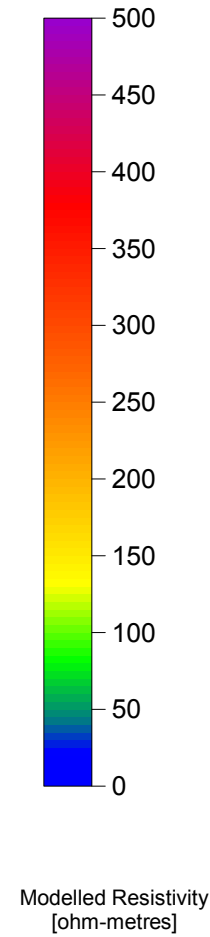
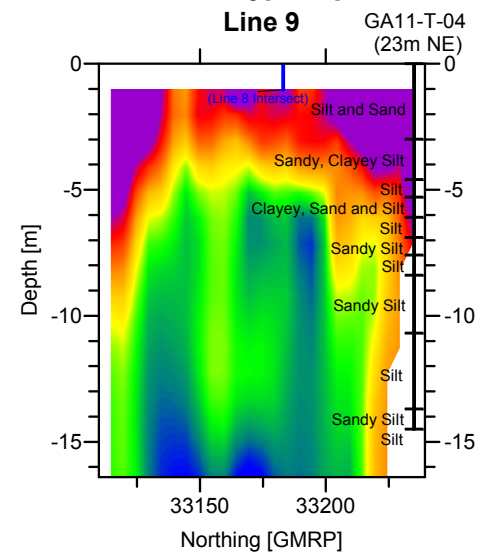
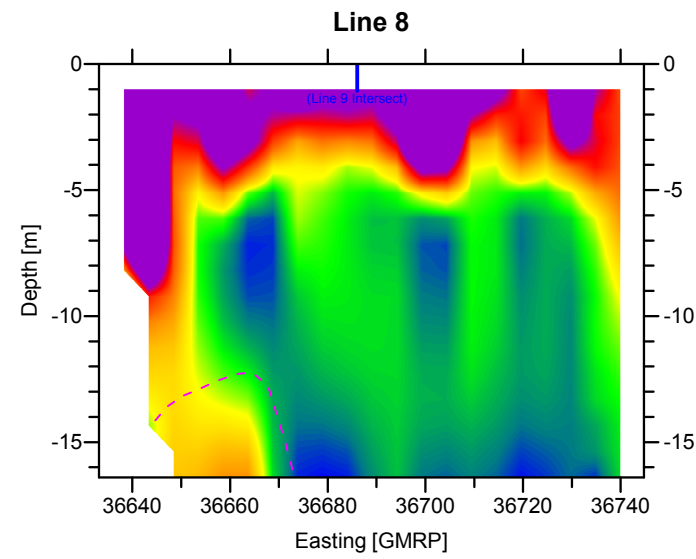
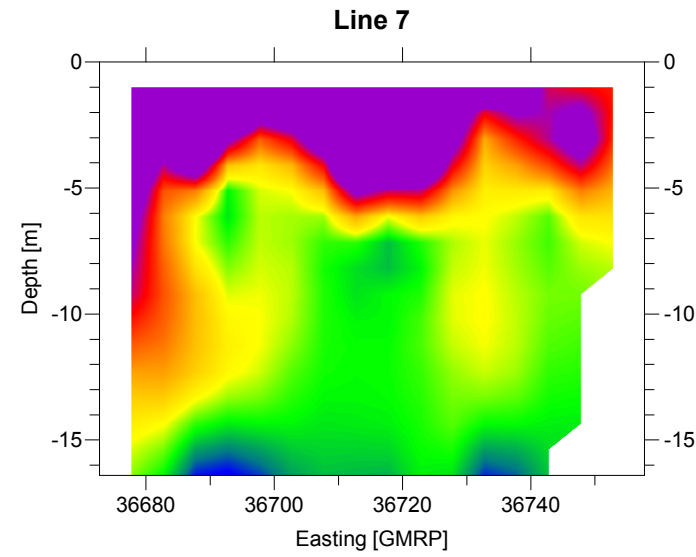
ATTACHMENT A
Figures A1 to A6

DRAFT




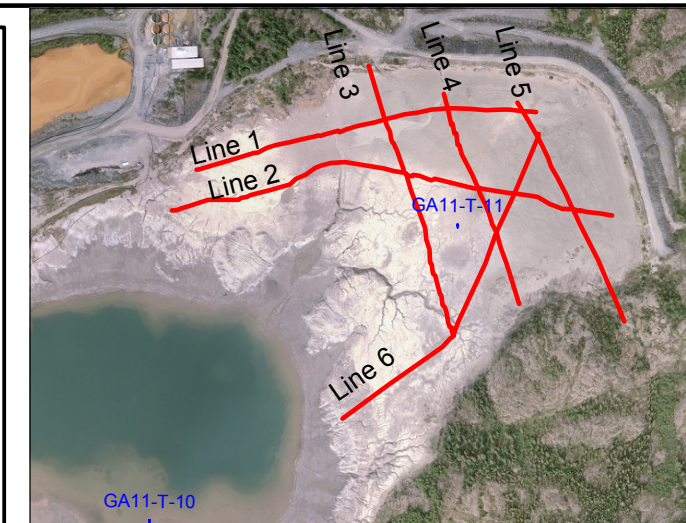
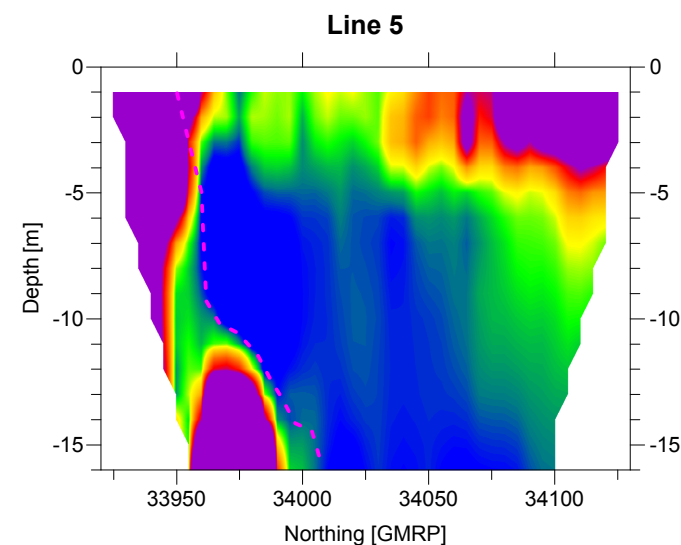
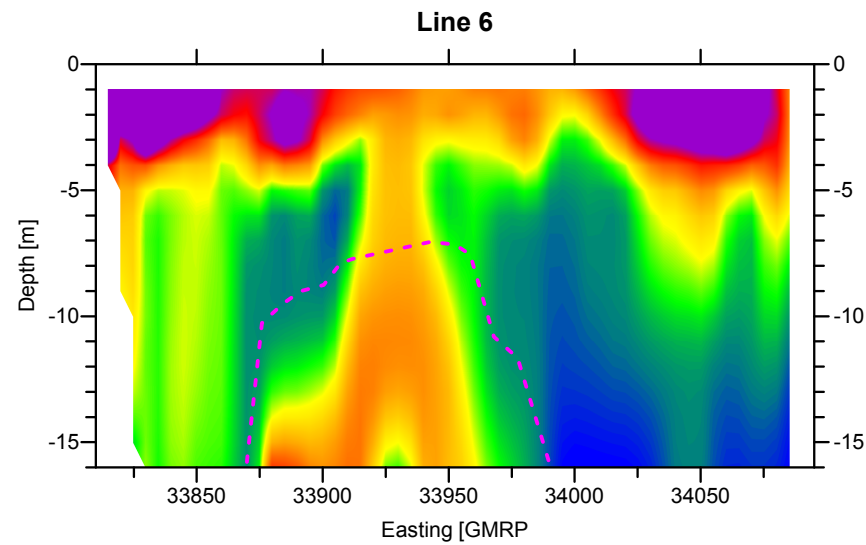
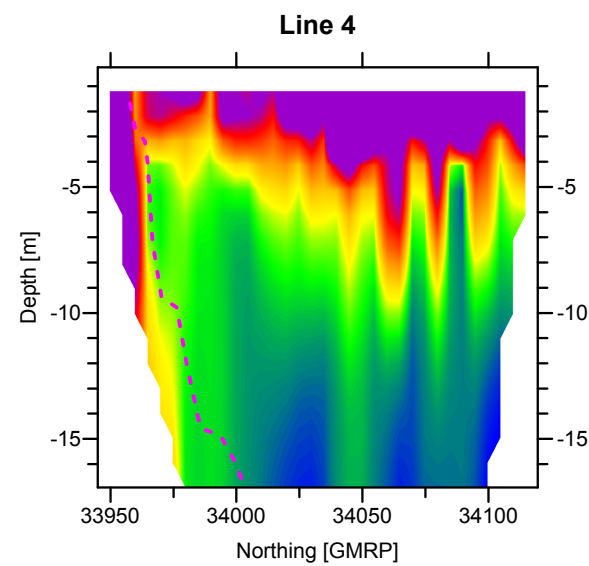
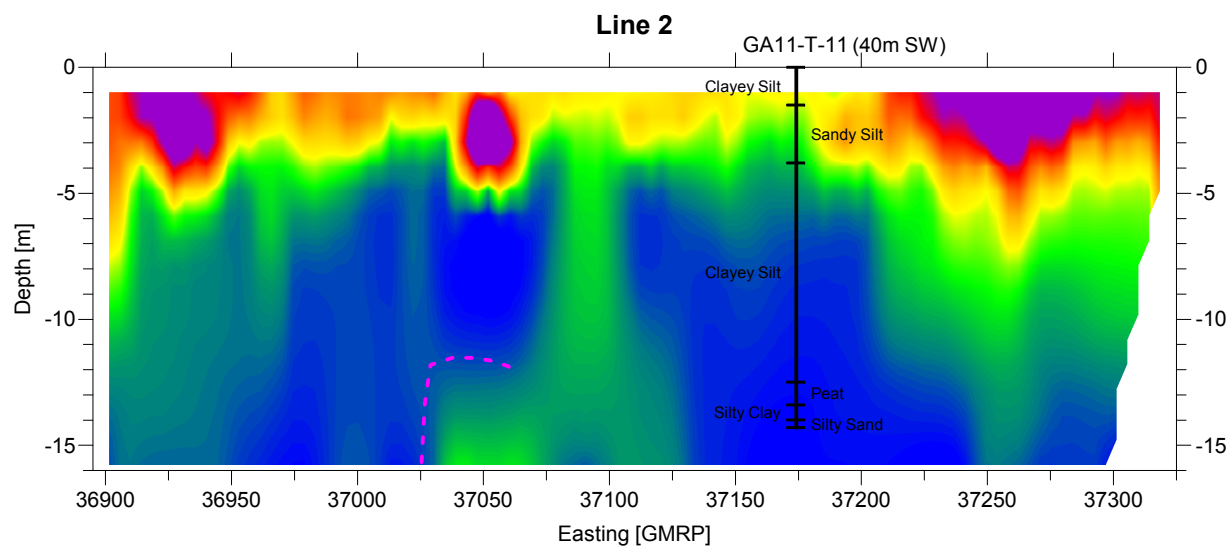
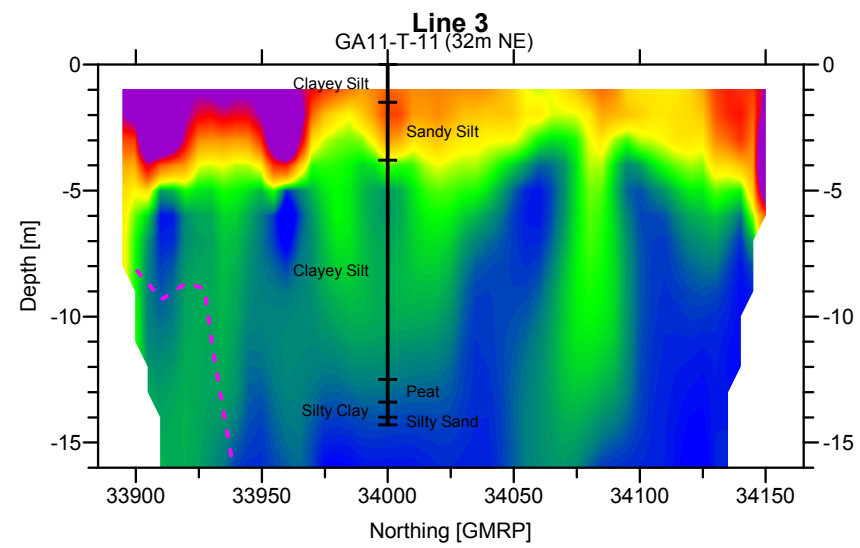
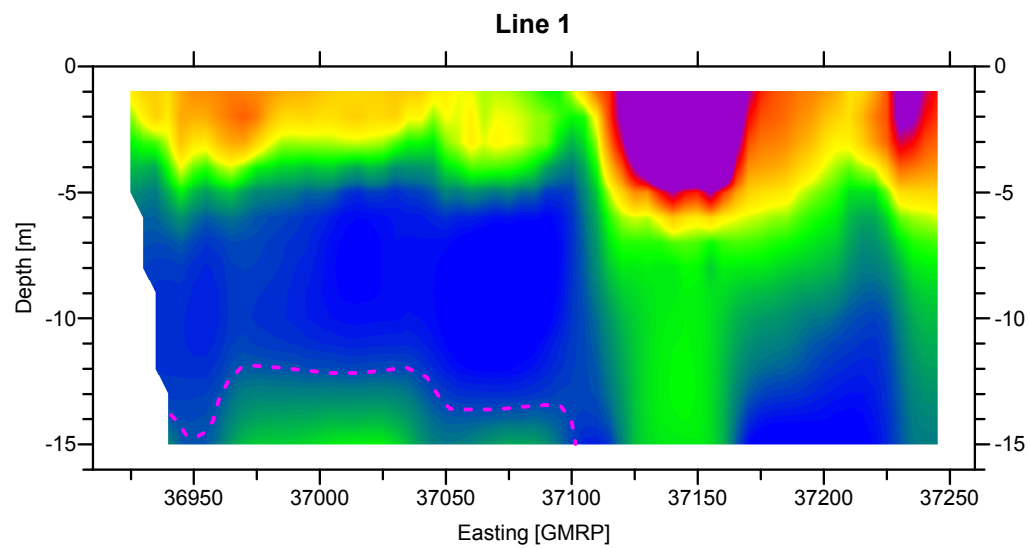
DRAFT

CLIENT	PWGSC Giant Mine, Yellowknife, NT			
TITLE	Geophysical Investigation Tailings Storage Facilities (TSF) South Pond Modelled Resistivity Sections			
 Golder Associates Calgary, Alberta	PROJECT	13-1377-0115		
	DESIGN	SM	22APR14	SCALE AS SHOWN
	REVIEW	xx	28APR14	
			FIGURE: A1	

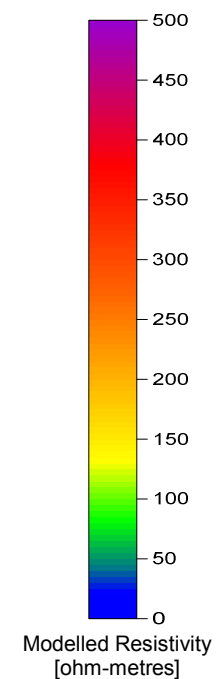



DRAFT

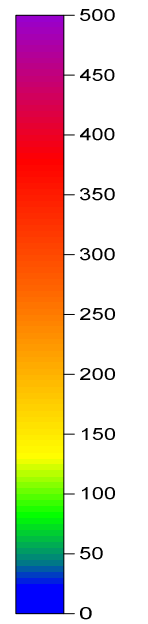
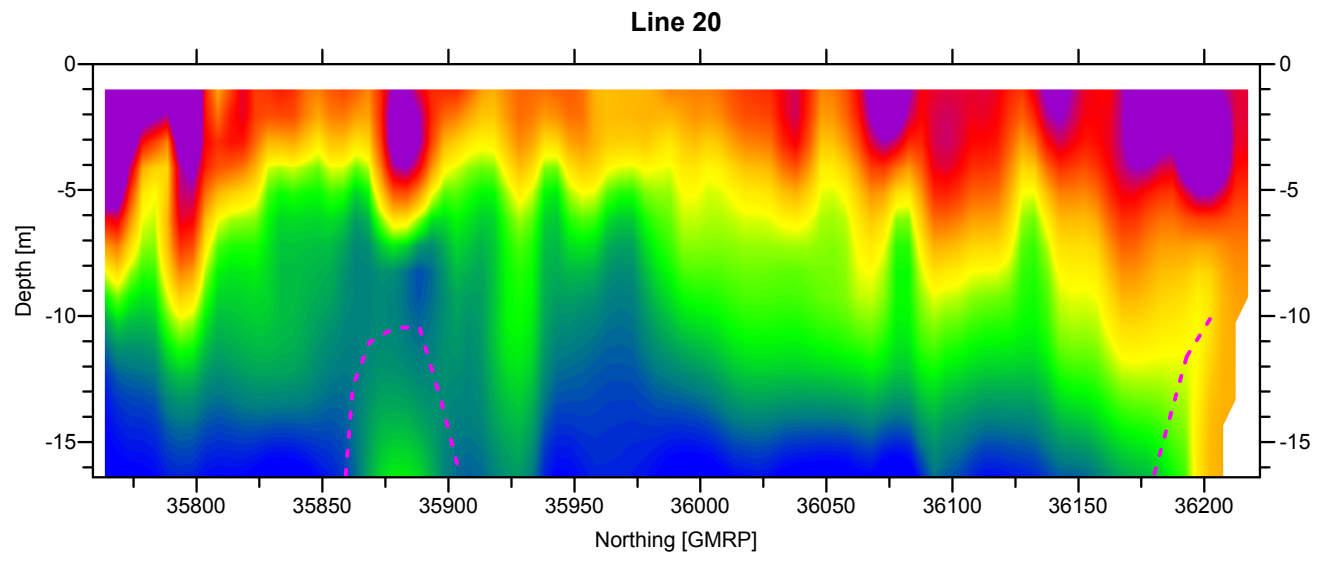
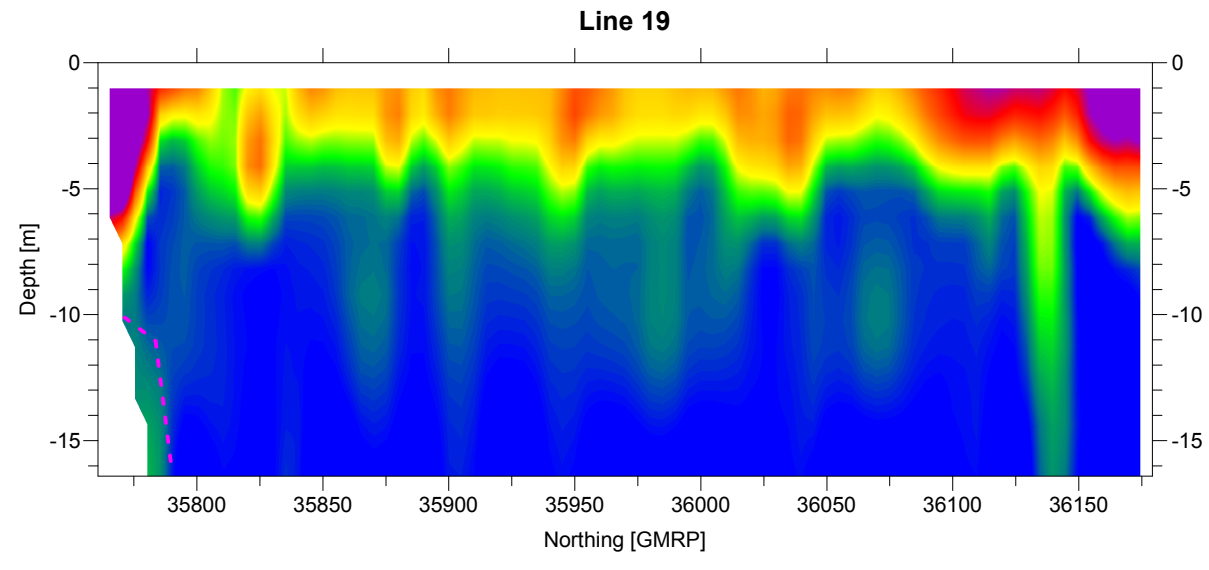
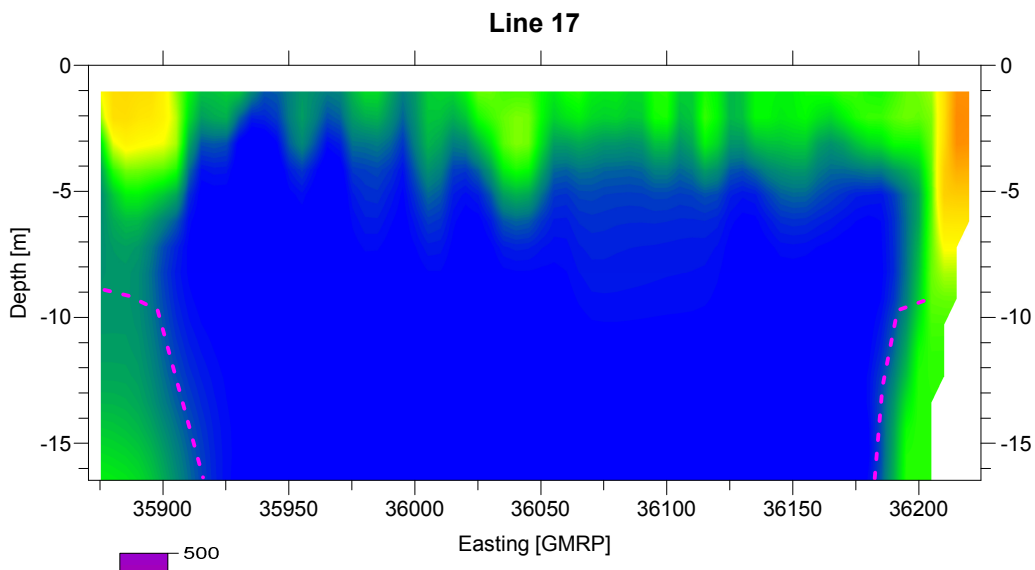
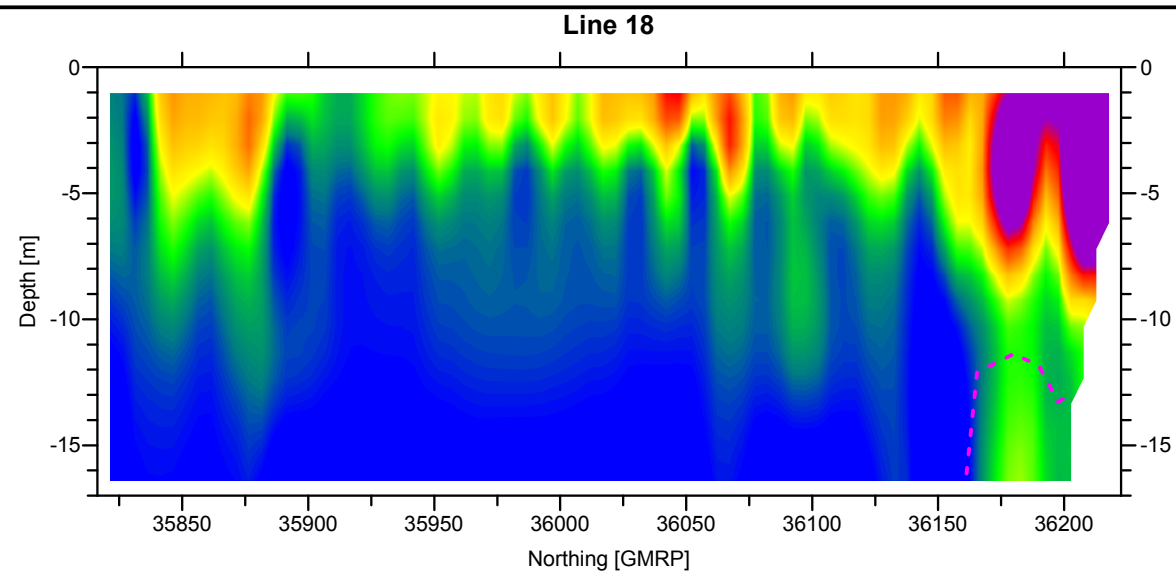
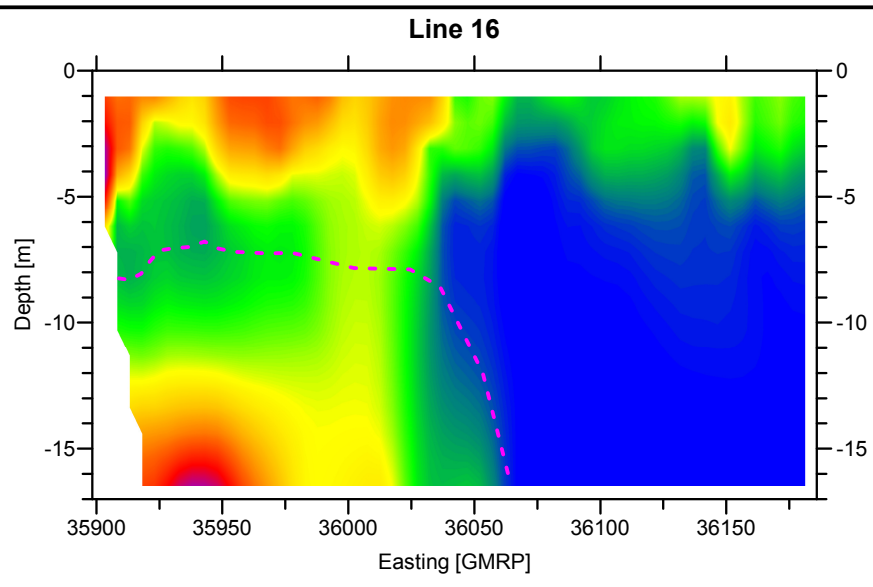
CLIENT	PWGSC Giant Mine, Yellowknife, NT		
TITLE	Geophysical Investigation Tailings Storage Facilities (TSF) Central Pond Modelled Resistivity Sections		
 Golder Associates Calgary, Alberta	PROJECT	13-1377-0115	
	DESIGN	SM	22APR14
	REVIEW	xx	28APR14
			SCALE AS SHOWN
			FIGURE: A2



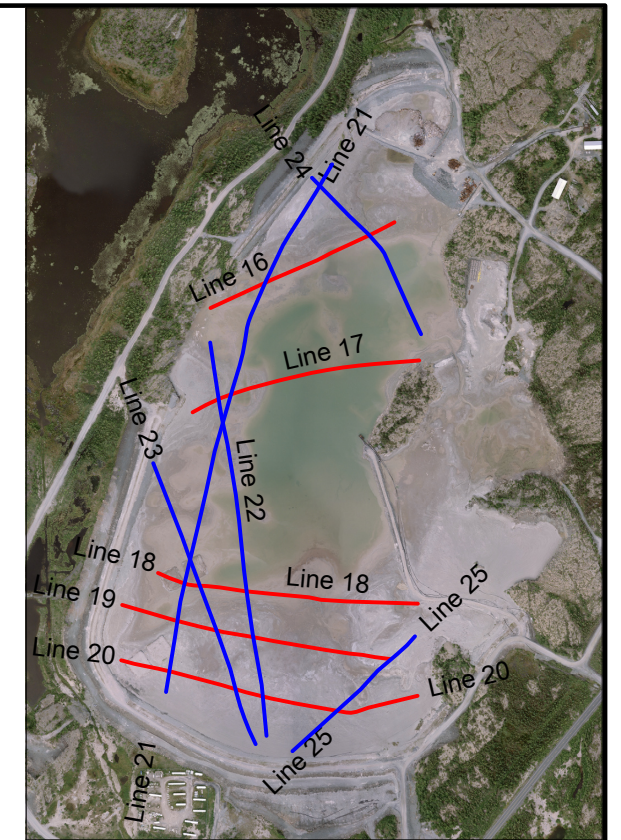
DRAFT



CLIENT	PWGSC Giant Mine, Yellowknife, NT		
TITLE	Geophysical Investigation Tailings Storage Facilities (TSF) North Pond Modelled Resistivity Sections		
 <p>Golder Associates Calgary, Alberta</p>	PROJECT	13-1377-0115	SCALE AS SHOWN
	DESIGN	SM 18APR14	FIGURE: A3
	REVIEW	MB 28APR14	




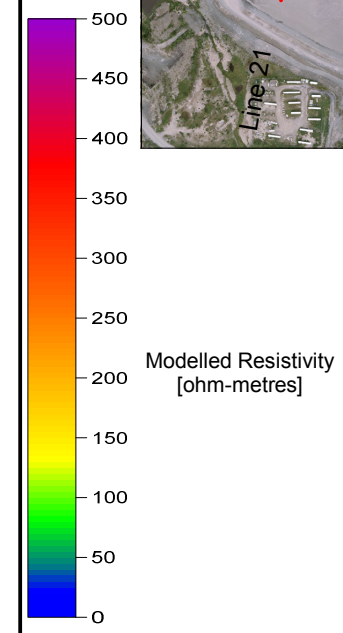
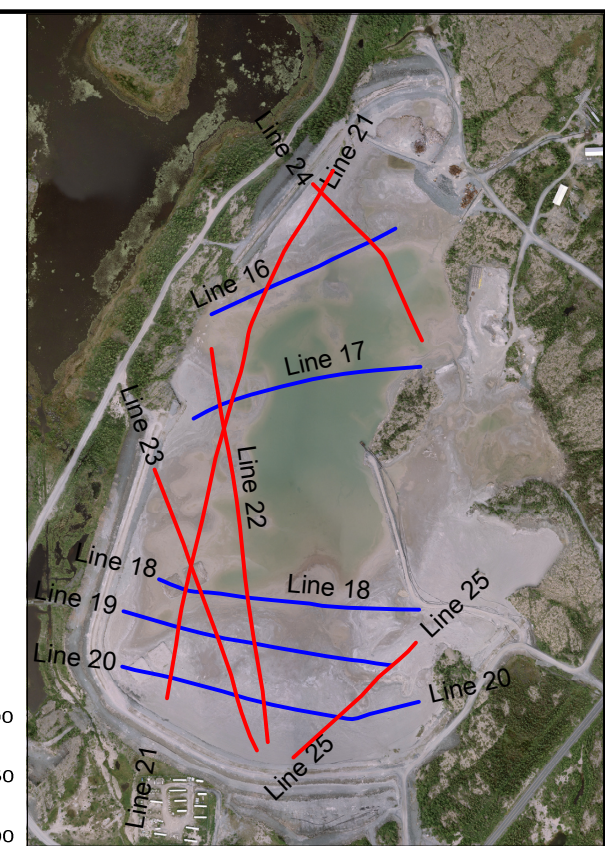
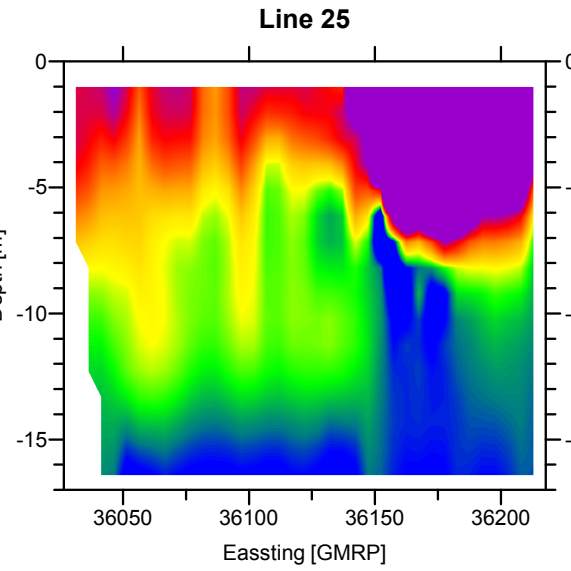
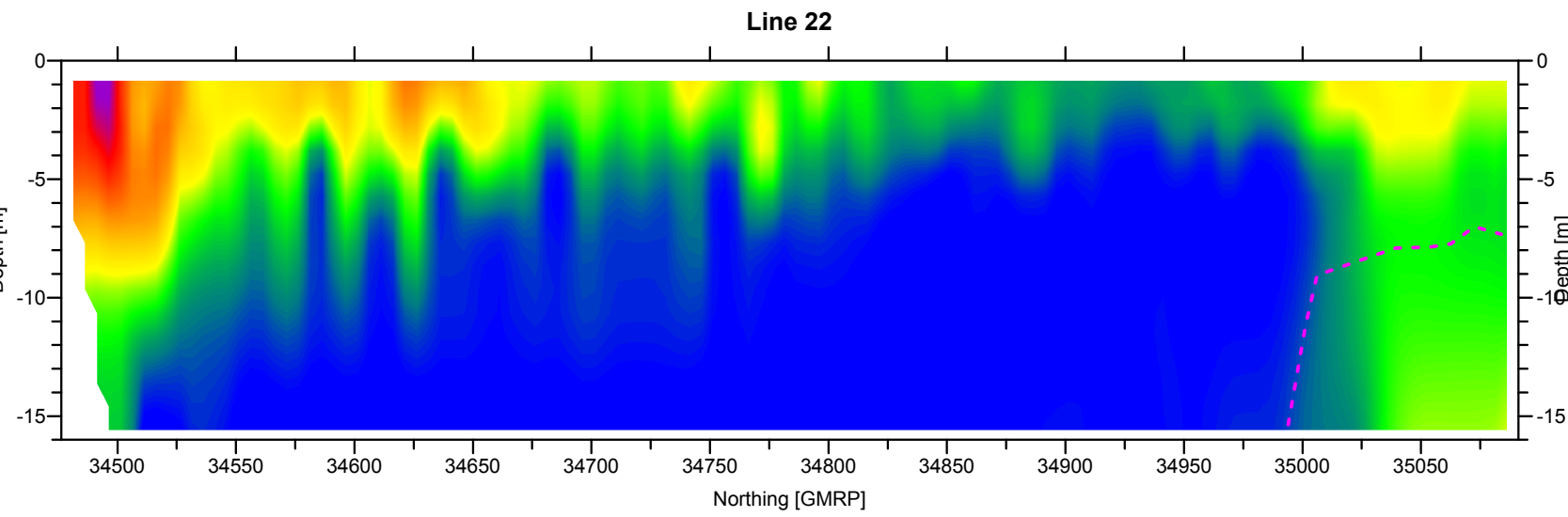
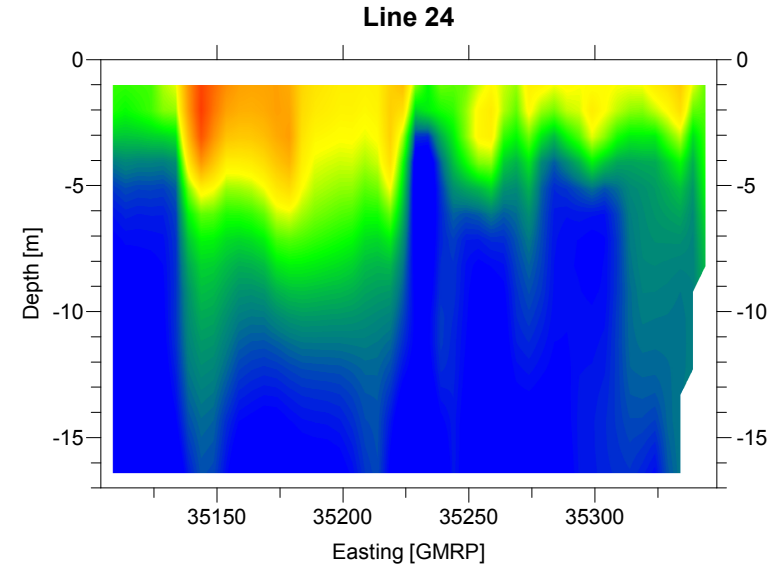
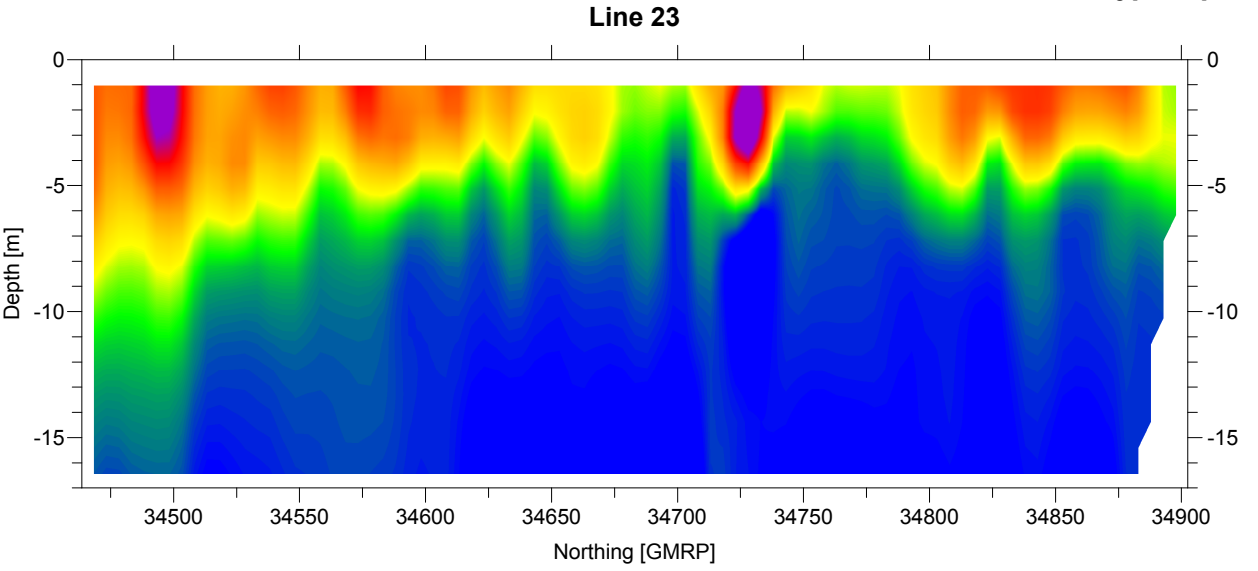
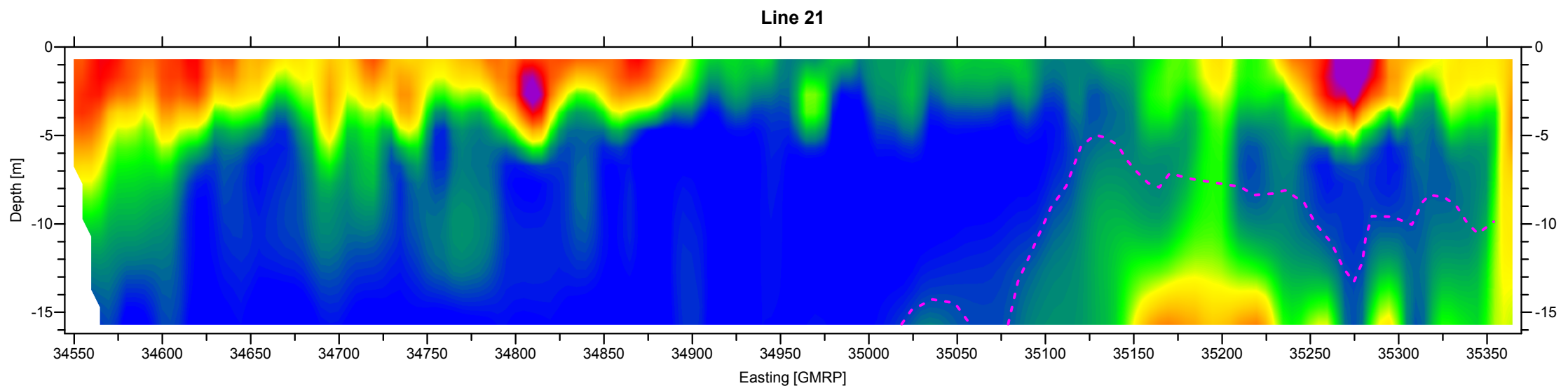
Modelled Resistivity [ohm-metres]



DRAFT

LEGEND
 — C-CERI GPS Survey Track

CLIENT	PWGSC Giant Mine, Yellowknife, NT		
TITLE	Geophysical Investigation Tailings Storage Facilities (TSF) Northwest Pond Modelled Resistivity Sections Line 16 to Line 20		
	PROJECT	13-1377-0115	
	DESIGN	LM 01MAY14	SCALE AS SHOWN
	REVIEW	MB 28APR14	
			FIGURE: A4



DRAFT

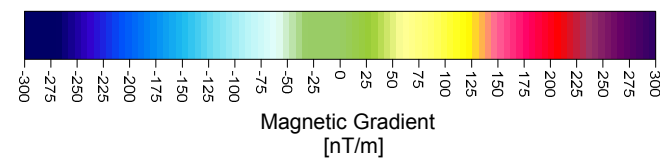
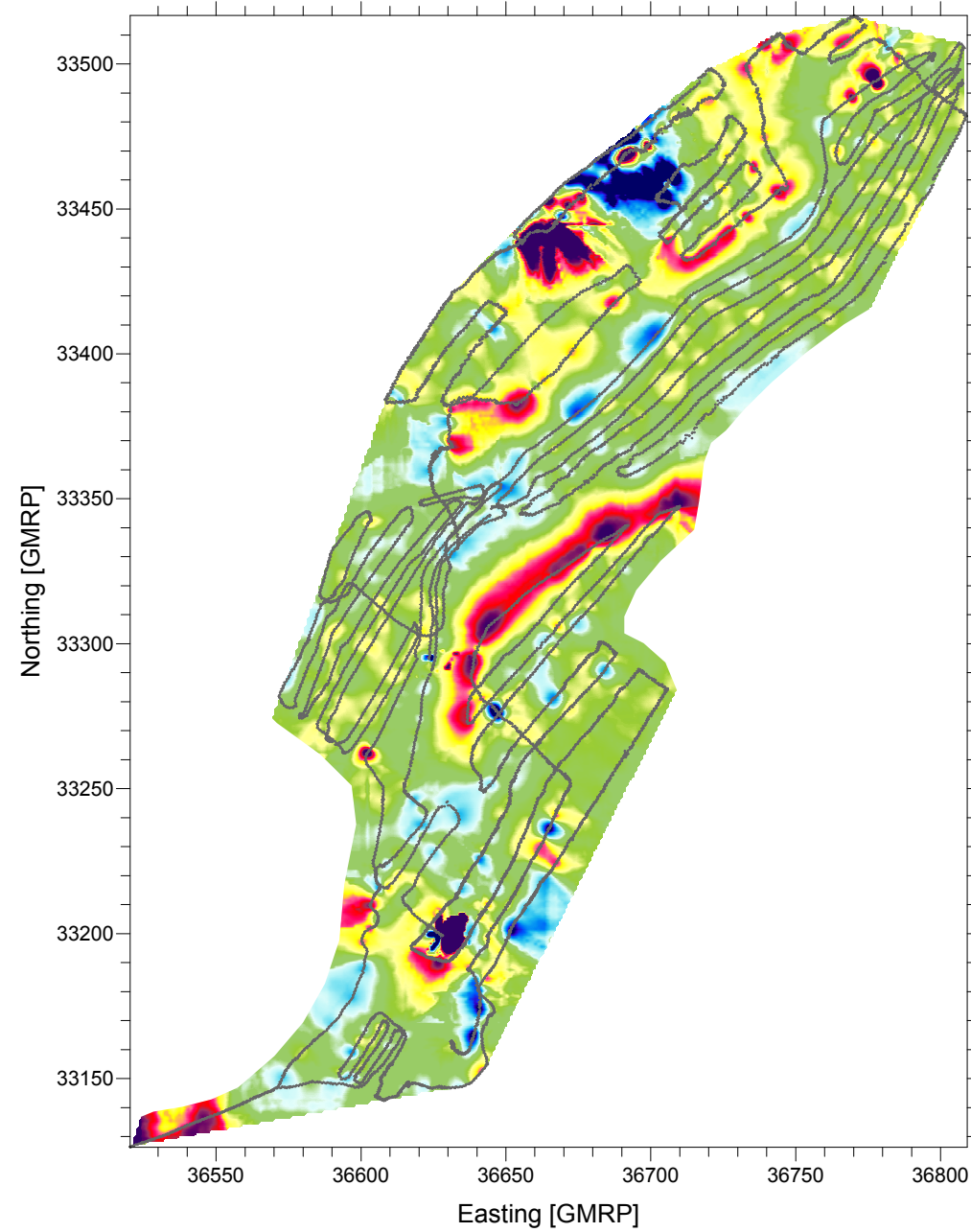
LEGEND
 — C-CERI GPS Survey Track

CLIENT
 PWGSC
 Giant Mine, Yellowknife, NT

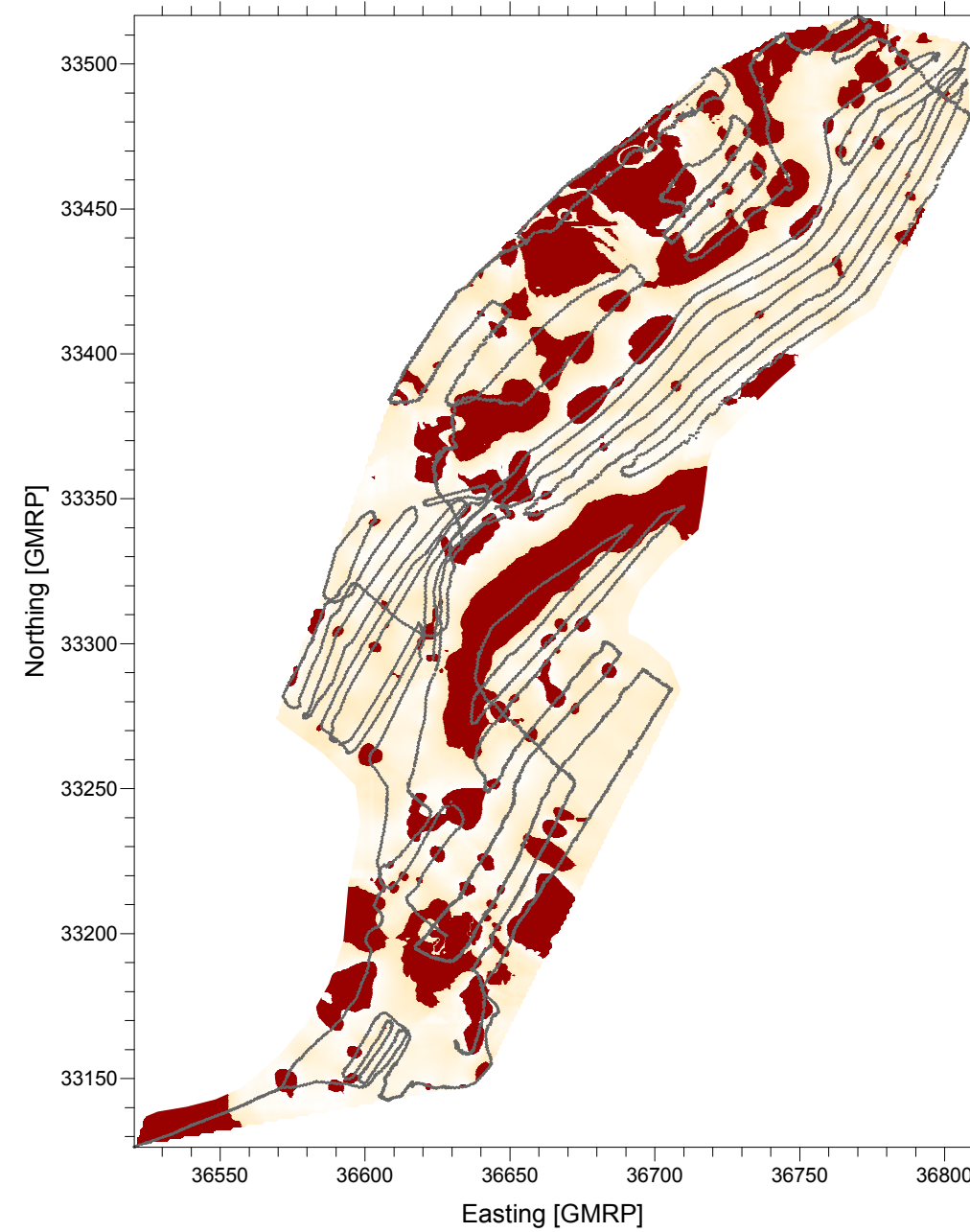
TITLE
**Geophysical Investigation
 Tailings Storage Facilities (TSF)
 Northwest Pond Modelled Resistivity
 Sections
 Line 21 to Line 25**


	PROJECT	13-1377-0115	SCALE AS SHOWN
	DESIGN	LM 01MAY14	
	REVIEW	MB 28APR14	
			FIGURE: A5

Measured Magnetic Gradient

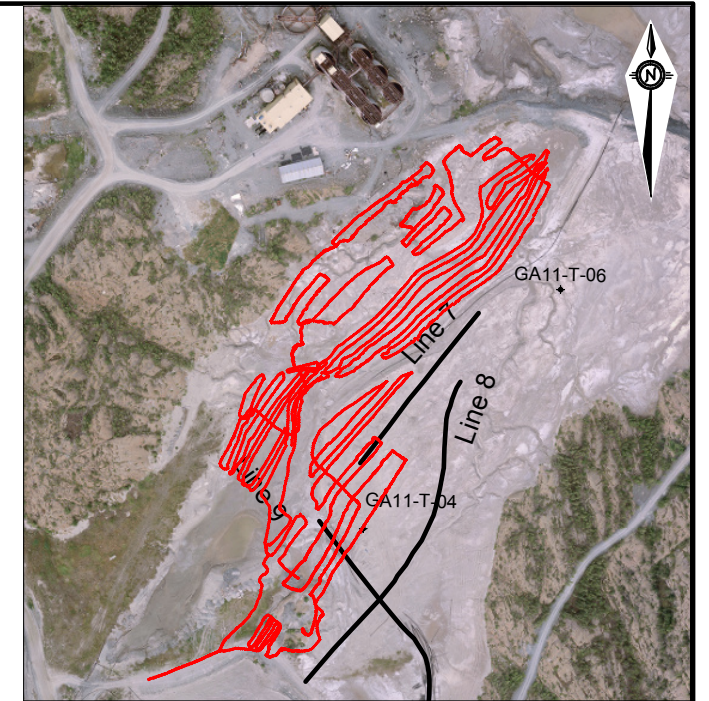


Interpreted Magnetic Gradient



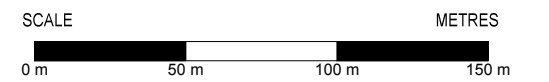
 Interpreted Location of Buried Metal

DRAFT




LEGEND

 Gradiometer Survey Track



CLIENT
 PWGSC
 Giant Mine, Yellowknife, NT

TITLE
**Geophysical Investigation
 Tailings Storage Facilities (TSF)
 Central Pond
 Vertical Gradient Map**

	PROJECT	13-1377-0115	SCALE AS SHOWN
	DESIGN	JG 22MAR14	FIGURE: A6
	REVIEW	MB 7APR14	